Introduction

Goals

The initial goal of this work was to generate a new optical fiber which could be used to obtain extremely efficient nonlinear interactions. The basic method used was to combine a structure which would result in very high optical intensities with a material which has a tremendously high nonlinear refractive index. The two approaches used for each of these tasks were, respectively, the holey fiber and fibers containing non-silicate glasses. In order to approach this problem, each task was addressed independently. My research work with each of these fibers also represents a significant increase in the state of the art for their respective applications. Some of the areas in which these fibers can be used are sensing systems, optical gain fiber (both Raman and more localized forms of gain), nonlinear applications, and low cost-short distance communications links.

With regard to random hole optical fibers, the goal of my research was to investigate methods, as needed, to develop a repeatable mechanism for fabricating microstructure fibers which are significantly different from the previously developed ordered hole fibers. The hope of this work was that such a structure will share many of the intriguing characteristics which have been found in ordered hole fibers. The work conducted under the heading of crucible technique fiber fabrication was intended to explore the question of whether it is

possible to incorporate core materials which have desirable properties into a predominantly silica fiber, despite the core material's extreme physical characteristics. In both cases, my target achievement was to fabricate samples of fiber which exhibited guidance of optical power over at least a short distance.

Background

Microstructured optical fiber

Holey fibers have been studied over the last several years because of their collection of properties which are very different from those found in conventional fibers. Typically, holey fibers are fabricated entirely of a single material, commonly bulk fused silica. Rather than doping the glass to obtain variations in the refractive index, holey fibers are produced by incorporating air holes into the cladding region.[1] The earliest related fiber was the "single material fiber" developed at Bell Labs in 1973.[2] In this case the core was a rod of silica which was suspended in the center of a large outer tube by a pair of thin bridges. A schematic of this structure can be seen in Figure 1. This is an example of the multimode sample of fiber. A single mode structure was also fabricated by using a much smaller core rod.

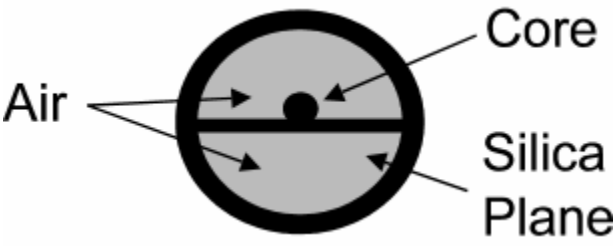

Figure 1: Schematic of "Single Material Fiber" from Bell Labs (1973)

Subsequent holey fibers have been developed to possess far more complex structures, including the photonic crystal fiber (PCF) which is a subset of microstructure fibers. In many cases this has been done by arranging a collection of tubes around a solid central rod. Through various techniques employed during the fiber draw, the structure of this preform is maintained.[1,3] The light which is guided in the solid core of these holey fibers experiences the inhomogeneous cladding as a nearly homogeneous material with an index of refraction which is a weighted average of that of the two materials (silica and air).

The most discussed property of the holey fiber is its ability to demonstrate single mode behavior over very large spectral ranges.[4,5] Individual fibers have been found to demonstrate single mode behavior over a range of wavelengths from 377 nm up to 1550 nm. This can be observed as resulting from the single mode condition for an optical fiber, in which the normalized frequency, $V = (2\pi\rho/\lambda)\left(n_{co}^2 - n_{cl}^2\right)^{1/2}$, must be less than 2.405. Due to the increase in the confinement factor of a fiber as one shifts to shorter wavelengths, less of the optical field extends into the air spaces within the optical fiber. As a result, the effective index of the cladding rises much more rapidly than would be

experienced in a conventional fiber. By properly selecting the ratio of the diameter of the air holes to their pitch, the single mode cutoff wavelength can be selected, independent of the overall scale of the fiber.

A similar argument applies to the usage of air holes for controlling the dispersion characteristics of the fiber. Zero group velocity dispersion has been reported at wavelengths as low as 765 nm, with anomalous dispersion occurring at longer wavelengths.[6] As a result, holey fibers become an intriguing host for a variety of optical processes which require either dispersion compensation or phase matching. Holey fibers can also possess multiple cores, and act as directional couplers, allowing the consideration of a host of device applications.[7]

Interest has begun to arise in the area of holey fibers which possess a random distribution of air holes. Theoretical analyses indicate that such random hole optical fibers (RHOFs) would exhibit properties which are very similar to those of ordered holey fibers.[8] Neither the traditional ordered hole fiber, nor the random hole optical fiber, is likely to demonstrate one property of the photonic crystal fiber. This property is the PCF's ability to guide light at both a high index defect of the structure (a solid core), or a low index defect of the structure (an air hole of different size than the others).[9] To obtain a photonic crystal fiber, the air holes are required to be periodically spaced. In the majority of these cases the periodic spacing occurs on either a triangular or hexagonal grid. In a few cases,

however, a photonic crystal fiber has been generated whose structure is radially arranged.[10]

Fibers containing non-silicate materials

An additional area of interest is fibers that contain non-silicate glasses. Although the vast majority of optical fiber development has been based on the ultra-pure chemical vapor deposited silica fibers (lightly doped with assorted elements), there has been prior work in fibers which are not silica based, for specialty applications. One such class of materials are the chalcogenide glasses which are used for transmission in the mid to long infrared region of the spectrum. Another potential application of the non-silicate glasses are in the field of fiber nonlinear optics. Silica is a material of tremendous strength, which makes it very desirable to use in fiber systems. Silicate glasses possess small nonlinear responses, however, which render it a less suitable host for nonlinear interactions. Some alternate glasses can have values of n_2, the nonlinear refractive index, which are fifty times that of silica, or even greater.

The disadvantages of fibers fabricated entirely from non-silicate glasses is in their intrinsically low physical strength compared to silicate glasses, and in the difficulties involved in merging them into a standard telecommunications style of optical fiber. All of these materials have melting temperatures which are far lower than those found in silica, and coefficients of thermal expansion (CTEs) which are far greater.

Ideally, one would wish to be able to fabricate a fiber with the optical properties of the non-silicate glass, and the physical properties of silica. The natural approach to this is to construct a system in which the core is comprised of the specialty glass, enclosed in a surrounding region of silica cladding. This has been done extensively, with some materials. One such example is the inclusion of borosilicate-based stress regions in a polarization maintaining fiber, whether in elliptical geometry or in the PANDA structure. [11,12] Many of the non-standard materials, such as phosphate glasses, have not been possible to incorporate into a silicate fiber using existing techniques. When standard methods, based on chemical vapor deposition (CVD) or fusing of bulk glasses together, have been attempted, the result is a shattering of either the core or cladding, as the extreme difference in CTEs generates far more stress than the material can survive. A novel method, the “crucible technique”, has been developed for fabricating such fibers.

Overview of work

A listing of all preforms which were drawn during the course of this research can be found in Appendix A. It is noteworthy that while some of these preforms were drawn once, approximately half of them were drawn (or attempted to be drawn) repeatedly. These repeated attempts were to investigate whether altering draw parameters would result in either an improvement of the resultant fiber or, in some cases, would result in any fiber being successfully drawn from the preform in question.

The initial attempts at fiber fabrication were intended to see if a very straightforward approach to the end goal was possible. A set of ordered hole preforms were fabricated, constructed by the rod and tube method. The central cores of these preforms were replaced with high index Lead Indium Phosphate (LIP) glass. Following this, the preform was drawn into fiber. It rapidly became apparent that such a simplistic approach was inherently infeasible. Due to the extreme low melting temperature of the LIP glass, it became fully molten and flowed throughout all of the interstitial spaces of the preform. Thus, we determined to attempt to separate the two problems and work on each of them independently, with the possible goal of recombining the results at the end. A flow chart showing the development of the parallel research avenues can be seen in Figure 2.

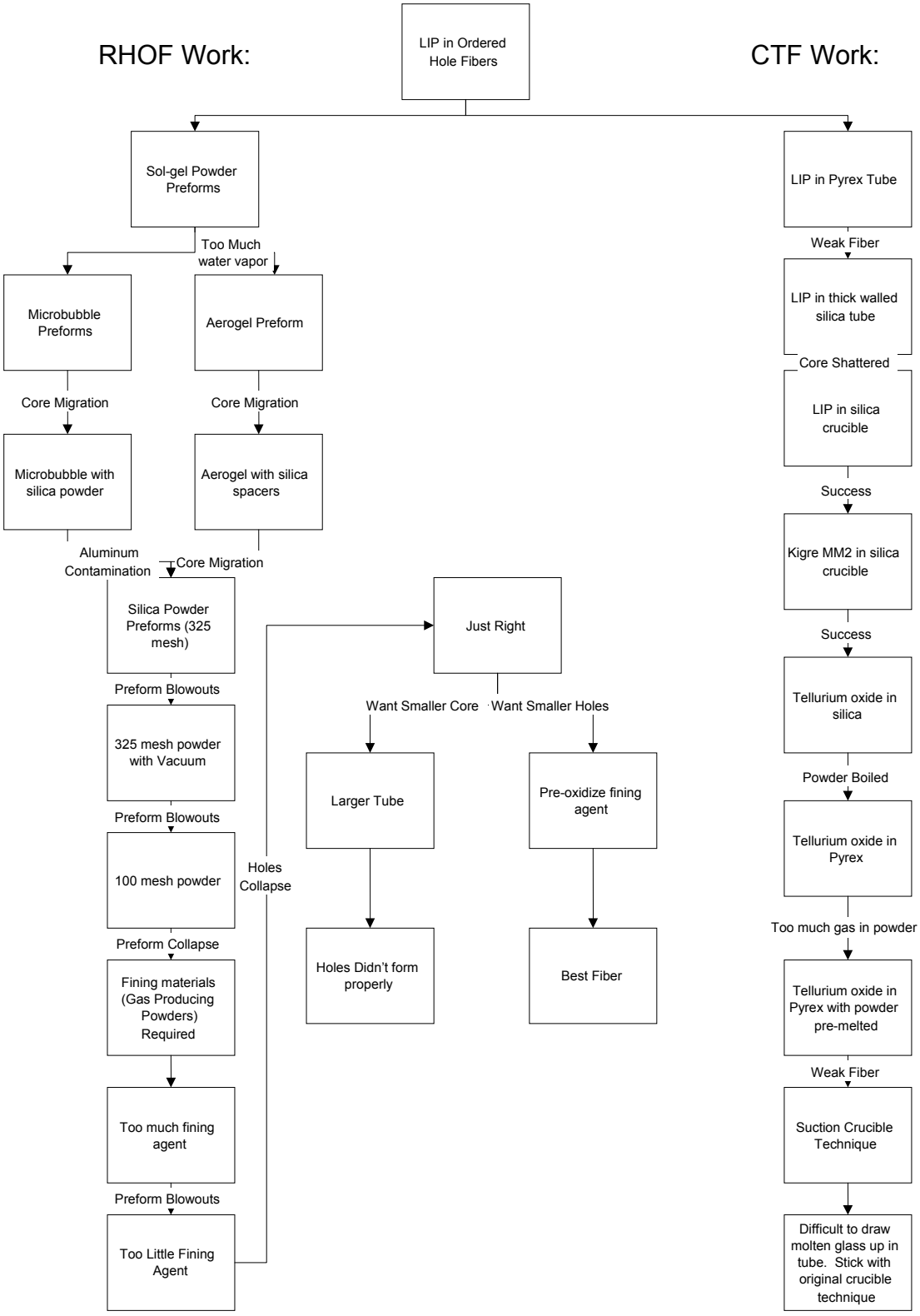

Figure 2: Research Flow Chart

This document will first cover the research in microstructure optical fiber, beginning with a survey of the major varieties of microstructure fibers, followed by a discussion of the random hole optical fiber (RHOF). Then will follow a discussion of the measurement of the properties of these fibers. Next, I will cover the development and theory of the non-silicate crucible technique fibers. Last will be some example applications of the fiber types developed in this work. Appendix A gives a comprehensive list of all preforms drawn in the course of this research. Appendix B contains an overview of some of the salient points of operation of a fiber draw tower. Appendix C presents a description of a method for measuring the refractive index profile of a fiber with extremely high delta.

References:

[1] J.C. Knight, T.A. Birks, P.St.J. Russell, and D.M. Atkin, "All-silica single-mode optical fiber with photonic crystal cladding," Optics Letters **21**, 1547-49 (1996).
[2] P. Kaiser and H.W. Astle, "Low-loss single-material fibers made from pure fused silica," Bell. Syst. Tech.J. 53, 1021-1039 (1974).
[3] Patent: DiGiovanni, et. al. "Article comprising a micro-structured optical fiber and method of making such fiber," Patent Number: 5,802,236 (Sep. 1, 1998).
[4] T.A. Birks, J.C. Knight, and P.St.J. Russell, "Endlessly single-mode photonic crystal fiber," Optics Letters **22,** 961-963 (1997).
[5] J.C. Knight, T.A. Birks, P.St.J. Russell, and J.P. de Sandro, "Properties of photonic crystal fiber and the effective index model," Journal of the Optical Society of America A **15**, 748-752 (1998).
[6] J.K. Ranka, R.S. Windeler, and A.J. Stentz, "Optical properties of high-delta air-silica microstructure optical fibers," Optics Letters **25**, 796-798 (2000).
[7] B.J. Mangan, J.C. Knight, T.A. Birks, P.St.J. Russell, "Dual core photonic crystal fiber," CLEO (1999).
[8] T.M. Monro, P.J. Bennett, N.G.R. Broderick, and D.J. Richardson, "Holey fibers with random cladding distributions," Optics Letters **25**, 206-208 (2000).
[9] S.E. Barkou, J. Broeng, and A. Bjarklev, "Silica-air photonic crystal fiber design that permits waveguiding by a true photonic bandgap effect," Optics Letters **24**, 46-48 (1999).
[10] G. Vienne, Y. Xu, C. Jakobsen, H.J. Deyerl, T.P. Hansen, B.H Arsen, J.B. Jensen, T. Sorensen, M. Terrel, Y. Huang, R. Lee, N.A. Mortensen, J. Broeng, H. Simonsen, A.

Bjarklev, A. Yariv, “First Demonstration of air-silica Bragg fiber,” OFC ’04, paper PDP25.

[11] V. Ramaswamy, R. H. Stolen, M. D. Divino, and W. Pleibel, “Birefringence in elliptically clad borosilicate single-mode fibers,” Applied Optics **18**, 4080-84 (1979).

[12] S. C. Rashleigh and M. J. Marrone, “Temperature dependence of stress birefringence in an elliptically clad fiber,” Optics Letters **8**, 127-129 (1983).

Classes of Holey Fibers

Holey fibers can be separated into three categories based on the degree of symmetry and order in the arrangement of the longitudinal air holes. These categories, in order of decreasing order and symmetry, are: Photonic Crystal Fibers (PCF), Holey Fibers (HF), and Random Hole Fibers (RHF). Each type of fiber has a different method of fabrication, as will be described below.

Photonic Crystal Fibers

The Photonic Crystal Fibers (PCFs) have the greatest number of restrictions on the location and size of the air holes. The spacing of the air holes in a PCF occurs entirely on the sites of a two dimensional lattice, in which every site is spaced according to a constant distance.[1] The PCF was the first reported type of holey fibers, and was produced through an extensive multiple drawing method.[1] Samples of two PCFs can be seen in Figure 3 and Figure 4. The first is an example of the original hexagonal pattern fibers. The second is what is referred to as a Bragg type of PCF, named with regard to the Bragg reflection which provides the confinement of the light.[2]

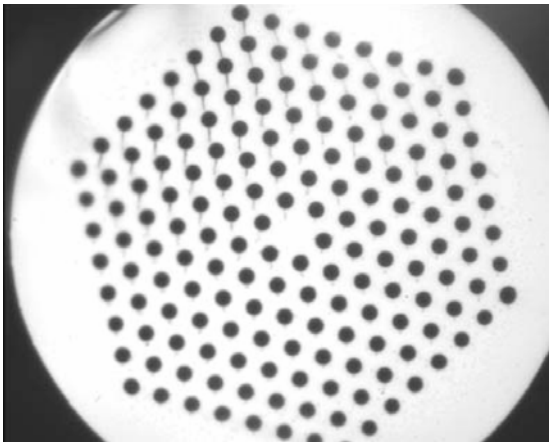

Figure 3: Micrograph of Photonic Crystal Fiber with Solid Core (The cladding diameter in this image is 268 µm)[3]

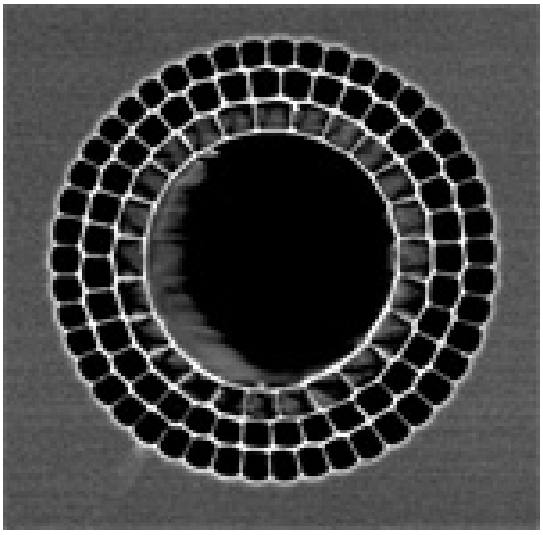

Figure 4: Micrograph of Photonic Crystal Fiber (Bragg Style) with Hollow Core[4]

The core of the fiber in Figure 4 is comprised entirely of air, highlighting one of the most important characteristics of PCFs. They do not guide the light by means of total internal reflection, unlike nearly every other variety of optical fiber. Instead they guide by providing a structure which is impenetrable for certain wavelengths of light, by ensuring that the various reflections of the different layers of silica-air boundaries add in phase.[5] This property is referred to as the photonic bandgap effect, and gives origin to the fibers' designation. A schematic

of how this can occur can be seen in Figure 5. The photonic bandgap is the collection of wavelengths at which the myriad reflections from the assorted air-glass boundaries add coherently, in a manner similar to what occurs in a dielectric stack mirror.

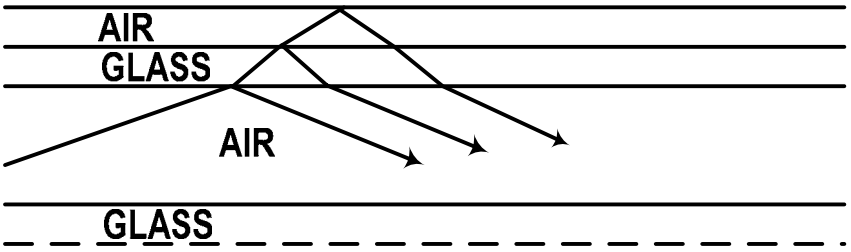

Figure 5: Schematic of Coherent Reflection inside a Photonic Crystal Fiber

Fabrication of Photonic Crystal Fibers

PCFs were initially fabricated by taking a thick-walled tube and milling a hexagonal cross section onto the outer surface.[1] The tube was repeatedly drawn down to obtain a cane possessing the same cross-sectional geometry. The canes are bundled with a single cane in the center which has a different geometry, typically solid, to construct the preform. An alternative geometry is to provide a central cane which has a hole which is different in size from those making up the rest of the preform, which can also provide a break in the structure's symmetry for the light to be guided within.[5] The overall preform would also have a hexagonal cross section. This preform would then be drawn into fiber in a fairly conventional manner.

An alternate method of producing PCFs was developed by Lucent Technologies.[6] Using a method which is more akin to producing holey fibers, they developed a system in which tubes were arranged around a rod in a closely packed hexagonal array. The top ends of these tubes were sealed off and an outer jacket layer of glass was collapsed around this array of tubes. These preforms would then be drawn at high temperature, allowing the spaces between the tubes to collapse by reducing the viscosity of the glass. As the draw progressed, the internal pressure in the tubes (from air that is trapped within them) would slowly rise until it was balanced by the inward force from the surface tension of the glass. At this point, the holes would remain open, resulting in a PCF structure.

Properties

PCFs derive their name from a set of peculiar optical properties which are derived from the highly ordered two dimensional structure which they possess. They are the only class of holey fiber which allows for guidance in a hollow core. Furthermore, as with other classes of holey fibers, the dispersion properties of PCFs are largely controllable via altering the hole diameter to pitch ratio.[7] The pitch is defined as the spacing between the center of adjacent holes.

In addition to being able to guide light in a hollow core, photonic crystal fibers are also capable of demonstrating endless single mode behavior.[8] This means that a given fiber can perform in a single mode fashion for any wavelength which the material can support.

Ordered Holey Fibers

There is one major difference between Ordered Holey Fibers (OHFs) and PCFs. Unlike the PCF, an OHF can only guide light in a region with a higher average index than the cladding. This is because OHFs do not exhibit the photonic bandgap properties described for PCFs. They do, however, benefit from being substantially easier to manufacture.[9] There are many different geometries of OHF. In some of these the fiber has interstitial holes which occur in the spaces where the adjacent tubes meet, in addition to those which are formed by the interiors of the component tubes.

Fabrication

OHFs are fabricated in a manner similar to that developed by Lucent to produce photonic crystal fibers.[4] A collection of tubes is packed around a central rod in a hexagonal array. An outer tube is collapsed onto the grouping of rod(s) and tubes to enable it to maintain its structure, and this preform is then drawn. Unlike the method described above for making PCFs, the tubes can be left open at the top, and the structure is held open by drawing the fiber at low temperatures. At this low temperature the high viscosity of the glass prevents the collapse of the air holes. When done with silica, the draw is extremely sensitive to a number of parameters, including the precise temperature of the preform in the furnace, the type of purge gas which the furnace uses, and the construction of the furnace's

liners. (See 'Effect of Furnace Properties on the Drawing of Holey fibers' on page 135.)

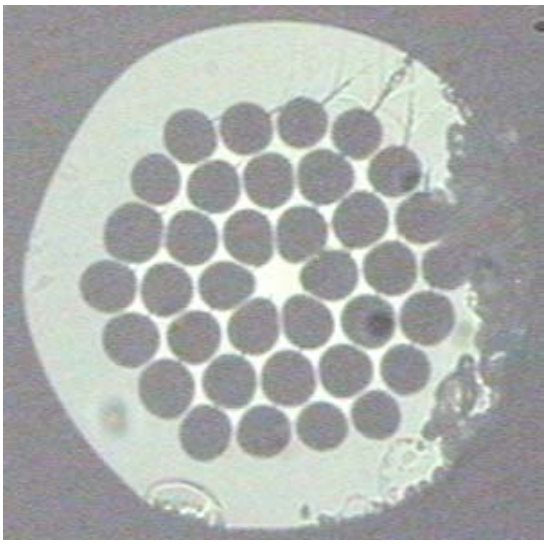

Figure 6: Optical Micrograph of OHF (Fabricated with Ismael Torres)

Properties

OHFs are believed to guide light exclusively through an effective index mechanism.[10] The effective cladding index is an average of the indices of the glass which forms the structure and the gas which fills the holes. This average is, in general, weighted depending on the degree of optical confinement to the regions comprised of glass.

There are numerous geometries which can occur in holey fibers. They can appear to have a structure similar to those found in PCFs, as is the case in the fiber shown in Figure 6. This fiber was fabricated from a hexagonal arrangement of tubes. One alternate geometry which is fabricated in holey fibers is called

"cobweb" fibers.[11] An example of such a fiber can be seen in Figure 7. In these fibers the tops of some, or all, of the tubes which form the structure are sealed, allowing the pressure to build up during the draw. This increased pressure causes these tubes to expand -- leaving large air holes with just thin filaments of glass in between.

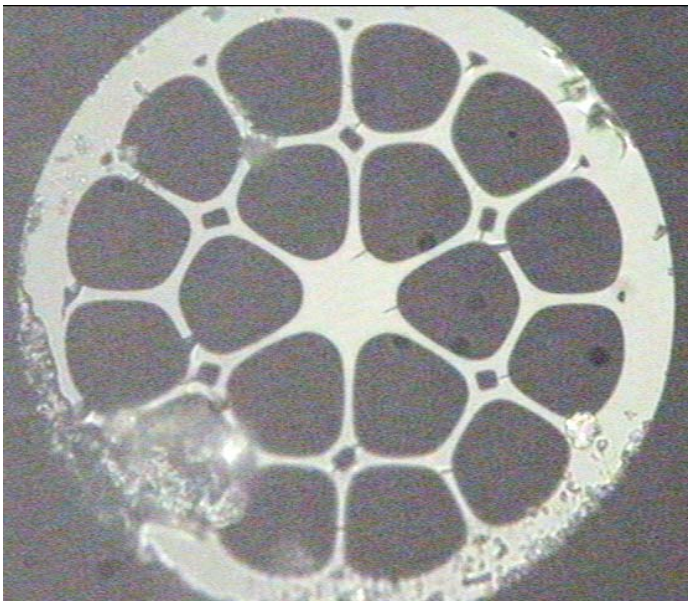

Figure 7: Optical Micrograph of Cobweb Style OHF IT 03-03 (Fabricated with Ismael Torres)

Development of Random Hole Optical Fibers

Random hole optical fibers (RHOF) were developed here at Virginia Tech, by Dan Kominsky, Dr. Gary Pickrell, and Dr. Roger Stolen. Unlike standard holey fibers, the holes in an RHOF are irregular in their location, as well as in their size, although the size distribution varies within certain ranges.

Successful RHOFs have a common structure. They have a solid outside tube which contains all of the elements and provides most of the structural strength of the fiber. There is a core region which is generally a solid piece of the same material used for the outside tube, although it can be replaced with a holey structure as well, as long as its index is higher than the surrounding cladding. Between these two regions is the cladding, sometimes called the “pore band.” The pore band is comprised, in general, of the same glass as the two other layers. In this material are holes filled with gas, but which can have a wide range of diameters. In the case of large holes, even the shape of the holes can be different, similar to the ‘cobweb’ OHFs described above.

The pore band can, in its simplest form, be a single layer. However, it can also contain multiple layers of different porosity, possibly separated by thin layers of solid glass.

Fabrication

A number of different methods were attempted to produce the random hole optical fibers. The attempts have been grouped by precursor material, in approximate chronological order to demonstrate the evolution of the fiber designs. The materials which were used for these attempts were: sol-gel derived glasses, crushed fused silica, microbubbles, and fused silica powders with gas producing materials. Only those fibers produced with a combination of silica powders and gas producing agents produced fibers which were successful at

guiding light, although some of the other techniques show promise, given further development.

Sol-Gel Techniques

Sol-Gel Glasses are manufactured through a process in which the glass is first formed via a chemical reaction in a liquid solution phase.[12] Preforms were fabricated both from monolithic pieces of sol-gel material, as well as from crushed sol-gel fragments. The initial sol-gel used for this experiment was an aerogel, which is comprised of approximately 3% silica and 97% air.[13] As a result, the average density of the glass is extremely low.

Several preforms were fabricated using the sol-gel material as a cladding. The initial attempt was a solid core surrounded by an aerogel monolith which has a hole bored through its center, along the long axis. The hole was just large enough to permit the 3 mm diameter rod to fit through it. When placed in the furnace, however, the preform came apart. Despite this, it was clear that the aerogel had condensed substantially into a much denser foam, with macroscopically visible air pockets. This indicates that the sol-gel material does have a structure which will allow it to form a pore band. All subsequent attempts occurred within the confinement of a silica tube because the aerogel's low density would not provide a robust enough surface for the exterior of the fiber. Sheathing all further fibers in the silica tube added to the mechanical strength of

the fibers, both by providing structural support and by making the outside surface of the fiber non-porous to reduce cracking from contamination or incidental contact.

The following preform, DK 01-03 was formed by concentrically fusing a core with the outside tube and filling the space between with chunks of aerogel. These pieces were irregularly shaped and had a maximum physical extent of approximately 1.5 cm. In the drawing process, the core migrated to the sidewall of the preform and fused there. An optical micrograph of this fiber can be seen in Figure 8. Another preform was tried where a monolithic block of aerogel was used in the same configuration as in DK 01-03, with similar results.

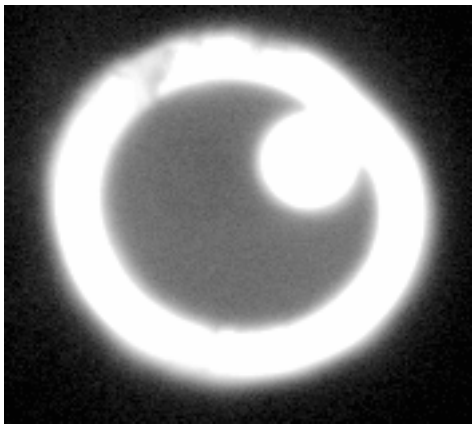

Figure 8: DK 01-03 Micrograph of Sol-gel Derived Fiber

A subsequent preform, DK 01-12 was attempted in which the pieces of sol-gel were separated by thin disks of fused silica which had been threaded onto the central core, in an attempt to force the core to remain well centered in the

preform. A micrograph of this fiber can be seen in Figure 9. As occurred in DK 01-03, the core is fused to the side wall, but the overall structure is deformed as well. The most likely explanation is that the aerogel did not provide sufficient support to prevent the silica disks from tipping around the core. Because these disks would initially be fused to the surface of the outer tube in a single place, the tipping of the disks would pull the side wall in, resulting in the kidney shape seen in Figure 9.

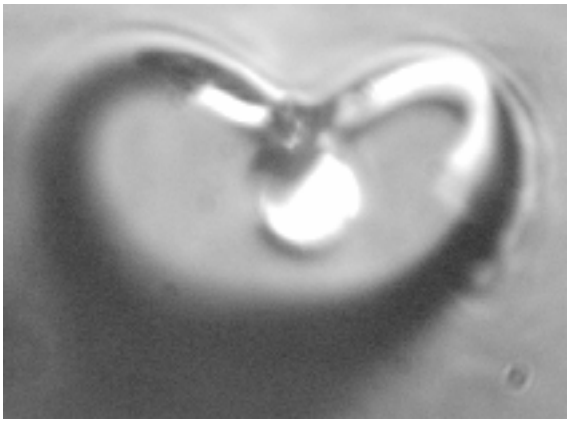

Figure 9: DK 01-12 Micrograph of Sol-gel Derived Fiber Containing Silica Spacer Disks

The aerogel-based work made it clear that the material which is used to form the cladding needs to be of sufficient density to prevent the core from migrating though the fiber during the draw phase. Aerogels, due to their extremely low density, are not suitable in this regard. Furthermore, when the aerogel is exposed to the temperatures needed to draw a silica fiber, the material densifies, resulting in a much smaller volume of glass containing area and a very large region entirely filled with air.

While it may be possible for a sol-gel based cladding to be used successfully to produce a random hole optical fiber, it would need to be of much higher density than the aerogels used in these experiments. Based on the successful structures of later, powder based preforms, I would estimate the necessary density of the sol-gel used to form the preform would have to be somewhere in a range greater than 90% that of silica in its initial state (before it is exposed to the high temperature of the fiber draw). In this range the density may be high enough to prevent core migration.

Powder Preforms

The Powder Preform method of producing holey fibers, unlike nearly all other methods of preform fabrication, starts with a structure which is not a monolithic piece of glass. Neither is it based on a collection of glass monoliths as in the rod and tube construction of ordered hole fibers. Instead, the core, which is a solid rod of glass (generally silica,) is surrounded by a region of fine particulate glass. When this assembly is placed into the furnace, the powder fuses, leaving a large number of air holes at the point where the grains were not initially in contact. These vacancies are then drawn out into tubes when the fiber is drawn from the preform. This has been attempted first with sol-gel derived powders, then with powders that are obtained through the crushing of bulk fused silica with collections of microbubbles, and finally with powders that are mixtures of microbubbles with crushed fused silica.

Sol-Gel Powder Preforms

Four preforms (DK 00-06, DK 00-09, DK 01-04, and DK 01-07) have been fabricated using sol-gel derived silica powder in the cladding. The sol-gel powder is a very pure, very uniform silica which has microporosity on the scale of nanometers.[14] The intention of these preforms is to generate a random hole cladding which has exceedingly fine pores, on the scale of nanometers or less.

Several different issues arose when the sol-gel powder preforms were drawn. First, a large degree of consolidation occurred (as shown by the bait portions having large air pockets) estimated to be on the order of ten cubic centimeters. Secondly, these preforms have demonstrated a prolonged retention of moisture, even after being heated in a furnace to temperatures of 1000°C for up to eight hours. When the preforms were exposed to high temperature in the draw tower furnace, condensation formed in the upper regions of the preform. This moisture resulted in blow-outs of the preform. On the few occasions when this phenomenon was not too severe to preclude the fiber being drawn, a high degree of instability was present in the draw properties of the fiber. The tension and fiber diameter have varied widely, with the fiber often tapering off. These issues are commonly associated with variations in the thermal properties of the material or with variations in density. The broad range of tension indicates that the average temperature in the preforms taper is varying above and below the softening temperature of the material. This could be due either to variations in the material composition (which would alter the softening temperature), or to

variations in the density which would vary the temperature (as the same amount of heat being input to a smaller mass will result in a higher temperature).

Pure Fused Silica Powder Preforms

One preform was fabricated from crushed bulk fused silica. The powder was obtained by grinding scrap pieces of bulk fused silica in a mortar and pestle. This preform was assembled in the same manner as the above sol-gel powder preforms. An optical micrograph of this fiber can be seen in Figure 10. When the preform was drawn into fiber it almost totally collapsed, leaving just a few relatively large air holes and no evidence of the smaller vacancies which were intended. The location of the core is not evident, and the outside profile of the fiber is not circular, indicating a substantial redistribution of the materials during the draw.

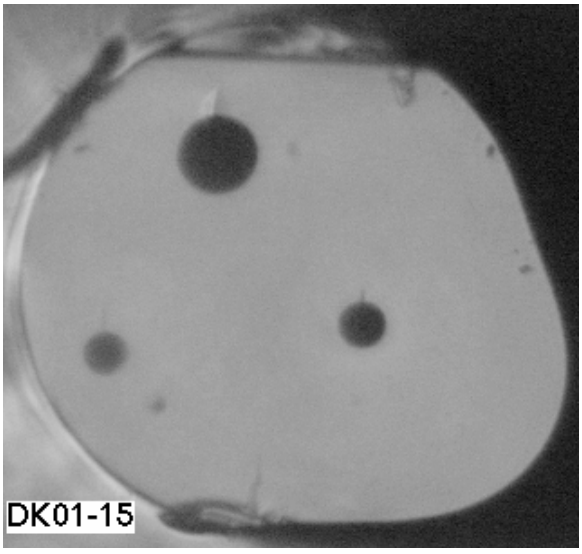

Figure 10: DK 01-15 Optical Micrograph of Fiber Produced from Hand Ground Fused Bulk Silica

A subsequent preform (DK 02-04) was tried using a commercially purchased 325-mesh silica powder. Initial attempts resulted in the core wandering around the fiber. Since this is believed to be due to insufficient density of the cladding material, attempts were made to try to make the powder more dense before further drawing this preform. The first attempt was made by simply attempting to tamp the powder with a glass rod. The fine material, however, was very difficult to efficiently pack in a preform, and there also were concerns about the ability to produce a consistent density of material.

Attempts to increase this density by successively applying vacuum and normal air pressure were also made (see 'Using Vacuum to Prepare Preforms' on page 45). However, too much air was retained in the powder. In addition, due to the fine nature of the material, the air which was within the powder did not have paths by which it could escape from the preform, resulting in pressurizing the preform. When the vacuum was initially applied, the powder was entirely sucked from the preform. This was later resolved by very slowly applying the vacuum while constantly tapping the preform in order to force the material to settle, thereby allowing the air to escape. The application of vacuum showed no discernable effect on the ability to draw the preform successfully.

Another attempt was made to densify the powder and eliminate the air contained within. After vacuum was applied to the preform, the preform was heated with an oxy-propane hand torch to cause the air to expand, thereby driving more air out

of the preform. Once the preform had reached a steady state, it was sealed, while maintaining the vacuum, by melting a chunk of Pyrex atop the powder region. This methodology was also unsuccessful since the preform still exhibited too much trapped air, and repeatedly suffered blow outs during the draw. The source of the air which caused difficulties in drawing the preforms made with 325-mesh powder are ascribed to a combination of two sources. First, the air is already present in the interstitial spaces, which is the result of the low packing density of the powder. Secondly, the air is adsorbed onto the surface of the particles and only liberated when the powder is heated.

Finally a preform was attempted using 100-mesh silica powder. In this case, no effort was made to densify the powder beyond tapping the preform after the powder had been added. A vacuum was applied to this preform, with no evidence of air trapping, and the preform was never sealed. The air holes in this fiber collapsed almost completely, a behavior similar to what occurred with the silica chunk preform. A micrograph of this can be seen in Figure 11. It appears that if one uses a powder as coarse as the 100-mesh, it is necessary to include some other source of air to prevent the total collapse of the cladding region.

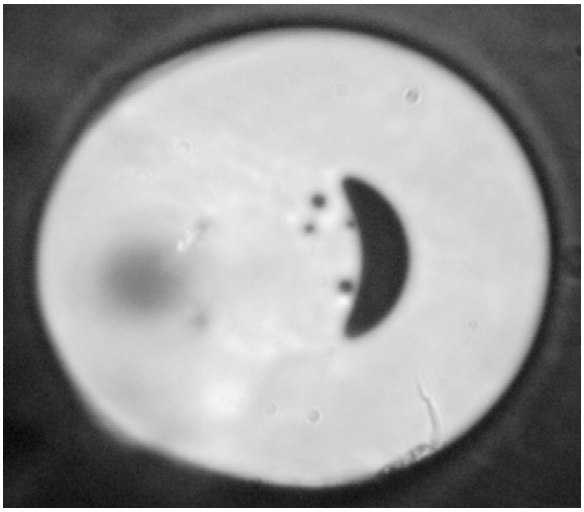

Figure 11: DK 02-05 Optical Micrograph of Fiber Made with 100-mesh Silica Powder

Microbubble Preforms

One possible approach to incorporating air into a powder is through the use of microbubbles. The microbubbles are hollow spheres of glass which have diameters in the one to ten micron range. Our theory was that the interstitial air would be eliminated, while the air which is contained within the microbubbles would be retained, forming the basis of a holey fiber. A series of preforms were fabricated where the air holes were created by including prefabricated microbubbles to the silica powder.

Microbubble Preforms

Two preforms (DK 01-08 and DK 01-09) were attempted in which the cladding was constructed exclusively of microbubbles. These microbubbles are hollow, air-filled spherical shells of glass with diameters of approximately five microns.

The microbubbles are fabricated from aluminosilicate glass. When these preforms were drawn they exhibited some properties associated with photonic crystal fibers, including a highly frequency dependent transmission function. Bulk samples of the bait had an opalescent appearance.

Similarly to the aerogel fibers, the core in these fibers was observed to have migrated until it was fully in contact with the outer tube wall, rendering the fiber unsuitable for use as a transmission medium. As in the case of the aerogel preforms, this migration is believed to be the result of insufficient density in the cladding of the fiber. In order to resolve this problem, we decided to attempt a series of preforms which used a mixture of microbubbles with silica powder.

Crushed Silica/Microbubble Preforms

Due to the tendency of the microbubble preforms to allow the core to fuse to the tube wall and the crushed fused silica preforms to collapse, a new series of preforms were fabricated by mixing the microbubbles with the crushed fused silica powder (DK 01-14 and DK 01-16). The initial preform of this type, DK01-14, consisted of 33 percent microbubbles, by volume. An optical micrograph of the fiber can be seen in Figure 12. As can be observed in the micrograph, the core of the fiber, while still off axis, has not fused entirely into the outer jacket wall. The migration of the core again indicates that the cladding material is insufficiently dense. It can also be observed in Figure 12 that the cladding is highly inhomogeneous. This may be due to the wide distribution of the silica

particle size which was used in fabricating the preform. There are also regions where the index is higher than that of the core. This is likely due to the aluminum content of the glass, which is known to raise the refractive index of silica.

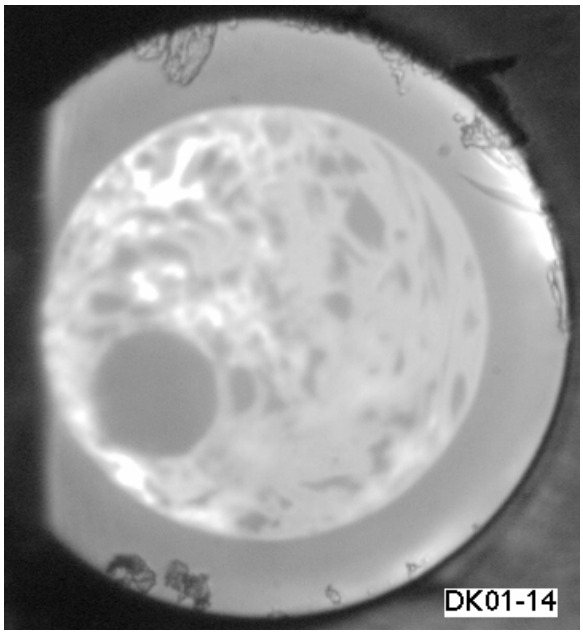

Figure 12: DK 01-14 Mixed Microbubble and Crushed Fused Silica Preform

A second preform (DK 01-16) was fabricated with 10% microbubbles, by volume. This preform was less successful than the previous one, exhibiting problems associated with excess air trapping. The preform had numerous blowouts during the draw, and showed an uncommonly low tension during the draw.

The ideal method for producing mixed microbubble-fused silica preforms seems to involve the use of microbubbles which are formed entirely of pure silica. By doing this, several potential issues are resolved, including the raised refractive index of the cladding, as well as greater assurance that the assorted materials share a similar working temperature. At the time that this work was under way,

however, no suitable source of pure silica microbubbles could be located. Due to the increase in refractive index from the aluminum content, this line of research was terminated. It was decided that, even if a sufficiently well-constructed fiber was drawn, the elevated cladding index would prevent the fiber from being useful because of the loss characteristics.

Crushed Silica Preforms with Gas Producing Materials

An alternate method for generating holes in a fiber was the inclusion of particles of a gas producing powder (GPP) into the crushed silica powder. These materials work by oxidizing at high temperatures. As the material oxidizes, it forms small bubbles. One possible application of this effect is to remove tiny air bubbles from batch melted glass.[14] The larger bubbles which are produced by the fining material gather the smaller bubbles as they rise through the molten glass. As such, these materials can be considered to be fining agents, although they differ in functional mechanism from the more conventional agents. As used in the holey fiber application, the bubbles are kept in the preform as it is drawn into fiber. This is referred to as in-situ bubble formation.

With the correct proportion of fining material and a suitable choice of glass powder, the fining material should be able to oxidize using the oxygen which is present in the spaces between (or adsorbed onto the surface of) the glass powder which comprises the majority of the material. One by-product of this reaction is the gas which is necessary to form the bubbles. The other by-product

of the oxidation of the silicon containing agent is silica glass. By choosing the size of the particles of fining material, it should be possible to control the size of the air holes which are produced inside the preform, and ultimately, the size of the holes which exist in the fiber.

The cladding material for these preforms was prepared by mixing measured amounts of the base silica powder with the fining material in a container. The container was sealed and heavily shaken for an extended period of time (at least ten minutes). Generally this shaking was done by hand, though when the container was rotated on a lathe, there was no discernable change in the fiber produced. Then it was poured into the cladding region of the preform. During the draw phase of the fiber preparation, three different primary processes are occurring. Firstly, the silica powder which forms the basis of the cladding is fusing into a single mass, preventing any generated gas from escaping. Secondly, the fining material is oxidized, releasing a gas, the composition of which is determined by the choice of fining material. Finally, all of the silica is softened, allowing the fiber to be drawn from the preform. As this is occurring, the spherical bubbles of gas which have been formed are drawn out into long thin tubules.

There are several characteristics which are common to fibers produced using In Situ Bubble Formation (ISBF). One is the random nature of the cladding structure. Unlike the ordered hole fibers, the pores in a RHOF are not

continuous over indefinite lengths of the fiber. Instead, the air holes can be seen to open and close, as the fiber progresses. The high number of holes, however, insures that at any given location along the fiber there is a sufficient density of air holes to maintain the light guiding characteristics. An optical micrograph of a section of bait off can be seen in Figure 13. This image was taken in a side view. In Figure 13, the light areas are the air holes and the dark regions are silica. Points A and B are the locations where, viewed from left to right, one air hole closes and another begins, respectively. Because this image is taken from a section of the bait, the aspect ratio of the tubes is much lower than would be anticipated in a completed fiber. In a sample of finished fiber, the holes are sufficiently long to make locating the end of a particular hole very problematic.

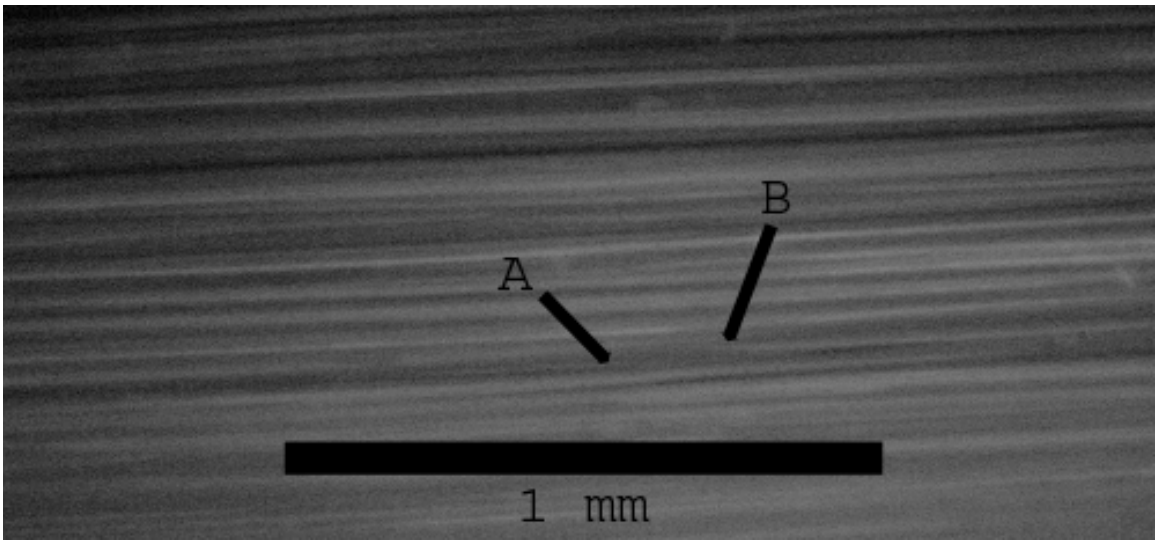

Figure 13: Side View Optical Micrograph of Portion of RHOF Bait Demonstrating the Opening and Closing of Tubules

Silicon Carbide

Preforms have been fabricated using a combination of Silicon Carbide and fused silica powder (DK 01-17, DK 01-18, DK 02-03, and DK 02-22). As the silicon carbide oxidizes, it produces the byproducts of silica and releases carbon dioxide gas. The first three preforms containing silicon carbide were mixed with a 325-mesh silica powder. Each was mixed with one percent (by weight) silicon carbide. The final preform was comprised of 0.083% silicon carbide, mixed with the 100-mesh silica powder.

The early preforms all possessed far too much fining powder. As a result, after these preforms were drawn into fiber, there were large areas of air with virtually no silica in the cladding at all. An optical micrograph of this can be seen in Figure 14. In addition, as the fiber was cooling, the drop in internal pressure resulted in partial collapse of the fiber. This can be seen in Figure 15.

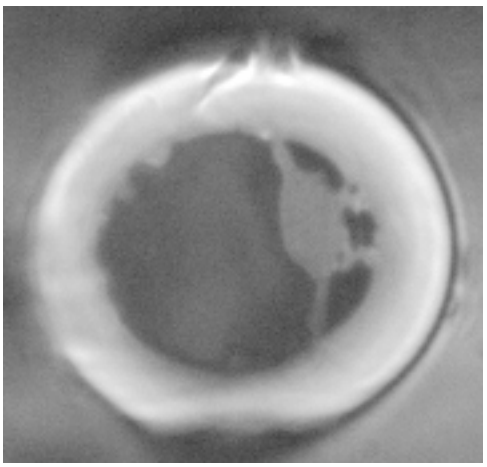

Figure 14: DK 01-18 Fiber from Preform with 1% Wt. Silicon Carbide

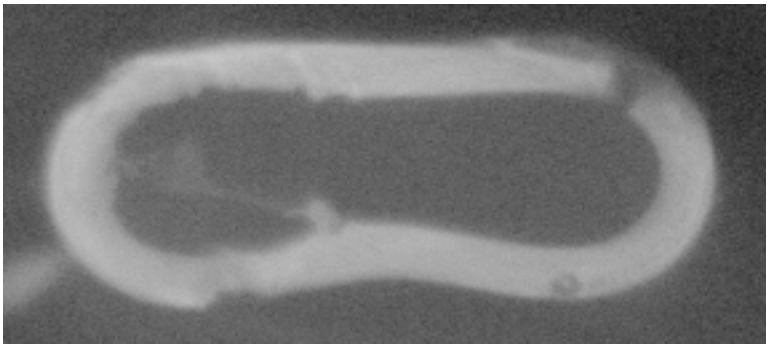

Figure 15: DK 01-18 Fiber from Preform with 1% Wt. Silicon Carbide, Demonstrating Flattening Due to Low Internal Pressure

In an attempt to resolve the issue of excessive air, a vacuum system was applied to preform DK 02-03 (see Using Vacuum to Prepare Preforms on page 45.) This did not seem to have any significant effect on the draw properties of the preform. Also evident in the early silicon carbide preforms was that the bait portion would change color from the initial white of silica powder to a dark gray. This was thought to be due to an insufficient amount of oxygen in the preform, resulting in an incomplete chemical reaction.

The final preform, which contained far less silicon carbide, with a weight percentage of only 0.083%, an order of magnitude lower still ended up producing far too much gas when drawn. As in the case of the earlier silicon carbide preforms, the bait off was darkened, and there were too many holes, resulting in an unstable fiber geometry.

Silicon Nitride

Silicon nitride (Si_3N_4) is an alternate fining material which oxidizes at a somewhat higher temperature than the silicon carbide, and releases nitrogen gas rather

than carbon dioxide. The initial preform of this type (DK 02-02) is comprised of 1% (by weight) silicon nitride mixed with 325-mesh fused silica powder. DK 02-02 was treated with vacuum to attempt to remove any excess air from the powder (see 'Using Vacuum to Prepare Preforms' on page 45). Once the powder had been evacuated to near vacuum, the top of the preform was sealed by melting a layer of Pyrex glass on top of the powder. Due to the large amount of fining powder used in this preform it was thought that reducing the level of ambient air would have little to no impact on the ability of the preform to be drawn. During the draw of the fiber, the air holes were far too large and, as with other preforms with excess air, DK 02-02 showed highly unstable draw properties. All later preforms which contain silicon nitride were fabricated using a 100-mesh silica powder. The coarser 100-mesh silica powder provided far better results, in spite of its lower purity.

The majority of the random hole fiber work was performed using silicon nitride, and all of the successful fibers were in that category. A listing of all preforms which contain silicon nitride can be seen in Table 1. There is a range of concentrations of silicon nitride from as low as 0.025 percent (by weight) to as high as one percent.

Table 1: Listing of Silicon Nitride Containing Preforms

Preform	Percent Weight Silicon Nitride	Core diameter (mm)	Tube (Inside Diameter x Outside Diameter) (mm)
DK 02-02	1% [a]	1	6x12

DK 02-06	0.5%	9	14x16
DK 02-07	0.5%	3	6x12
DK 02-08	0.25%	2.5	6x12
DK 02-09	0.1%	3	6x12
DK 02-10	0.05%	9	14x16
DK 02-11	0.05%	2.5	6x12
DK 02-12	0.025%	3	6x12
DK 02-13	0.075%	2.5	9x15
DK 02-14	0.04%	1	9x15
DK 02-15	0.075%	2.5	9x15
DK 02-16	0.06%	1	9x15
DK 02-17	0.075%	3	19x25
DK 02-18	0.075%	3	13x19
DK 02-19	0.05%	3	13x19
DK 02-20	0.075% [b]	2.5	9x15
DK 02-21	0.074%	3	13x19
DK 02-23	0.075%	3.5 [c]	9x15
DK 02-24	0.065%	3.5 [c]	9x15
DK 02-25	0.15% [d]	3.5 [c]	9x15
DK 03-01	0.1% [d]	3.5 [c]	9x15

Notes for Table 1:

a. Host powder is 325-mesh silica
b. Powder also contains 0.075% silicon nitride and 0.167% gold powder
c. Core material is composed of Saint Gobain high purity synthetic silica
d. Powder mixture was ramped up to 1000°C over one hour and then maintained at that temperature for 45 minutes before being put in preform

Although some of the preforms which contain amounts of silicon nitride in excess of 0.1% were drawn into fiber (notably DK 02-06 and DK 02-07), these fibers were not useful with regard to their optical properties. The highly irregular structures which were formed resulted in a total (or near total) lack of optical transmission.

One of the preforms which contained 0.5% silicon nitride was DK 02-07. A micrograph of the fiber drawn from this preform can be seen in Figure 16. In this

image, the air holes of this fiber are quite large and significantly distort the overall geometry of the fiber.

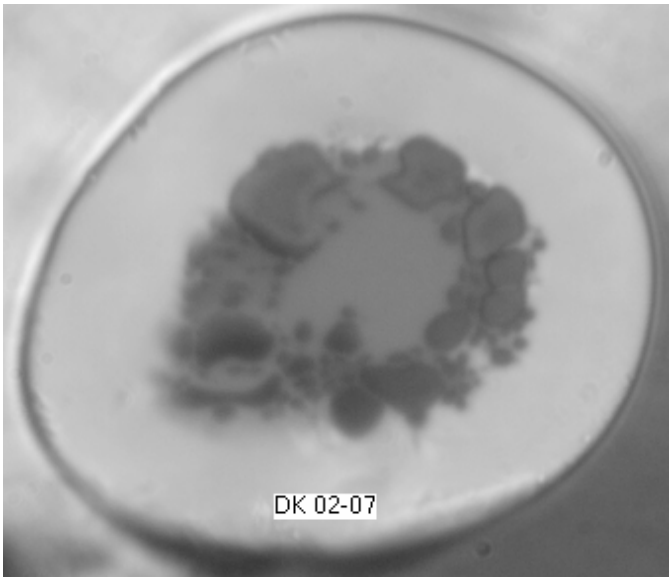

Figure 16: Optical Micrograph of DK 02-07

While this fiber comes closer than previous attempts to the desired structure, having an identifiable core and pore band, there is still an excessive amount of gas being produced. One of the postulated causes of the high loss evident in this fiber is an insufficient supply of oxygen within the preform resulting in a reduction reaction of the silicon species within the preform. A sample of a similar preform in which high loss was evident is shown in Figure 17, where the region of the preform in which the silicon nitride has oxidized is darkened. The reason why this is assumed to be the case, rather than simple contamination of the preform, is that when preform DK 02-05 (100-mesh silica without any silicon nitride) was drawn, there was no evidence of the darkening of the preform. We also know that it is not due to contamination of the silicon nitride, since a preform which

contained a larger amount of silicon nitride (DK 02-06), but is mixed with the 325-mesh powder, did not exhibit this darkening. One example of a preform which did not exhibit darkening is preform DK 02-04. Because the preform with the 325-mesh powder did not exhibit darkening, I believe that one of two phenomena are occurring. Either the additional air which is present with the finer powder (which was found to cause blow outs of the preform) is providing enough oxygen to fully drive the reaction, or there is another unknown contaminant in the 325-mesh powder, which somehow protects the preform from the darkening effect, in a manner similar to that in which the presence of hydrogen prevents photo-darkening.[15] The latter hypothesis seems rather improbable, based on the very few possible impurities which could possibly reduce a darkening effect. Furthermore, in later preforms where the percentage of silicon nitride was lowered, the darkening was absent.

Figure 17: Image of Preform DK 02-06

Preforms with concentrations of silicon nitride which are 0.05 percent or lower did not produce sufficient amounts of gas during the draw phase (Figure 18). There are two features which are immediately evident from this image. The first is the small number of air holes which are present. The other is the presence of the

large crescent shaped hole in the upper half of the image, separating the cladding from the outer tube. These crescent shaped holes appear in a number of different preforms, and seem to correlate with the temperature of the furnace, rather than with the amount of gas-producing powder.

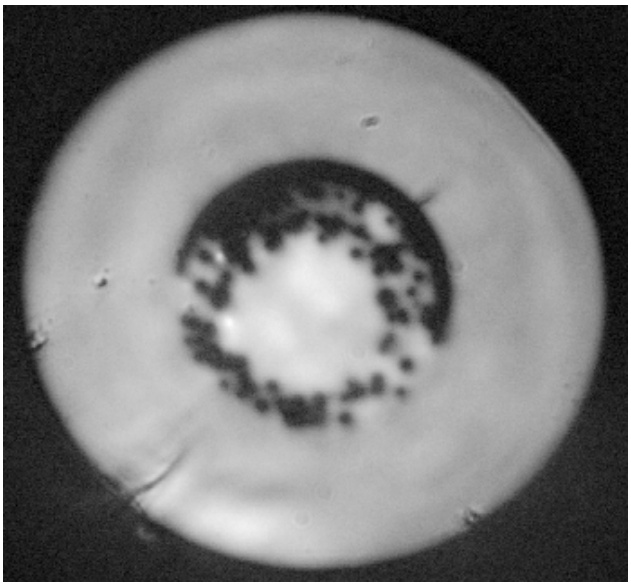

Figure 18: DK 02-11 Micrograph of Fiber with Insufficient Gas Producing Powder

When the draw temperature is high or, equivalently, the fiber tension is low, these crescent holes tend to form. They can be found at either the interface of the core and cladding, or at the interface between the cladding and outer tube. I hypothesize that these holes are caused by a tendency of the gases to migrate through the structure forming larger and larger air holes. Because the cladding is comprised of a powdered silica, it possesses pathways through which these gases can flow. The core and outer tube, however, are formed of either batch melt silica or, in some cases, deposited synthetic silica. In both cases this material is completely solid and impervious to gas flow, thereby creating a barrier

to the gasses. As a result, when the gas reaches these boundaries, it spreads laterally. This forces a separation between the solid surface of the tube and the region that was originally powder. Since this separation is defined by the surface of the "solid" region, the hole which forms has the crescent shape. An alternate explanation is that as the powder is heated and sinters, it is densifying and thereby occupying a smaller volume. If there are regions where the powder section does not fuse to either the outer wall or the core before this happens, the sintered powder can draw away from the solid surface, leaving the crescent shaped gap behind.

The preforms which were most successful in guiding light were (with one exception) those which had a silicon nitride concentration of 0.075%. The preforms with this composition seemed to balance the competing forces of surface tension and gas pressure. One example of such a fiber is DK 02-15 (Figure 19). Some evident features are the presence of a large number of holes (well in excess of a thousand), as well as a broad distribution of hole sizes. Some of the larger holes are approximately 7 microns in diameter, with the largest measuring 11.5 μm. In Figure 20 we can see a much higher SEM magnification of the same fiber. This image was taken with a magnification of fifty thousand. The smallest hole in that image is just under 105 nm across.

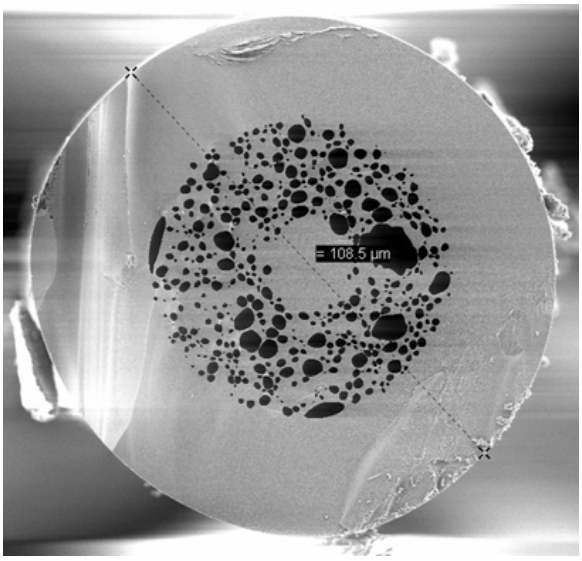

Figure 19: DK 02-15 Scanning Electron Micrograph of Fiber at 750X

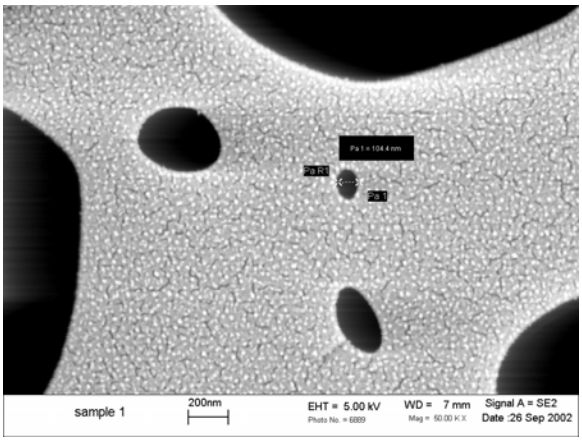

Figure 20: DK 02-15 SEM of Fiber at 50k Magnification

The final four preforms which have a silicon nitride containing cladding use a different material for the core than the previous ones. All of the early preforms used a bulk fused quartz rod for the core. This is a material which is formed by mining naturally occurring quartz, batch melting it, and forming it into rod stock. The final preforms (DK 02-23 through DK 03-01) use a synthetically fabricated

silica for the core rod. The material used for these preforms is Saint Gobain Spectrosil 2000. Synthetic silica is formed through a chemical reaction in the burning of a silicon containing compound (silicon tetrachloride, for example). The product of this reaction is a very pure form of silica, which in the case of Spectrosil is also high in water (hydroxyl group) content. The high water content is due to the reaction of the precursor chemicals in a flame (usually a hydrogen/oxygen flame). The primary benefit of synthetic silica is the reduced loss, which is a result of the much higher purity. The exception to this reduced loss is the absorption line caused by the hydroxyl group, which is centered at 1385 nm.

Two preforms (DK 02-25 and DK 03-01) were fabricated using a different preparation than the earlier preforms. The powder which would form the cladding of the fiber was mixed with a higher percentage of silicon nitride. This powder was then preheated in a furnace before it was placed in the preform to begin the oxidation process. The goal of this is to generate a greater number of smaller air holes. Since the oxidation process of the silicon nitride progresses from the outside of the particle towards the center and leaves behind a pure silica residue, the preheating results in each grain of silicon nitride becoming smaller and encapsulated in a thin coat of silica. Even at room temperature, the silicon nitride will slowly oxidize, resulting in the particles having a thin coat of silica on them, regardless of preheating. Thus the preheating effectively reduces the particle size of the silicon nitride.

The preheating was accomplished by putting the powder in an open silica bowl and placing it in a furnace. The furnace was ramped up to a temperature of 1000°C over the course of an hour and left there for an additional 45 minutes. The powder was removed from the furnace, allowed to cool rapidly, then placed in the preform.

The first preform fabricated with this powder was DK 02-25. With the understanding that each particle of silicon nitride would be generating less nitrogen gas, the initial weight percentage of silicon nitride was set at 0.15%. This was an excessively high amount, and resulted in the preform not generating useful fiber; the air holes were too large, and deformed the fiber, much as was seen in Figure 16. Following this the optimal preform of the project (DK 03-01) was fabricated by mixing eight grams of the powder from preform DK 02-25 with four additional grams of the 100-mesh silica powder. This yielded an overall weight percentage of silicon nitride of 0.1%. A micrograph of the fiber from DK 03-01 can be seen in Figure 21. Some of the important features are the significantly increased number of holes, as well as the smaller diameters of many of the holes.

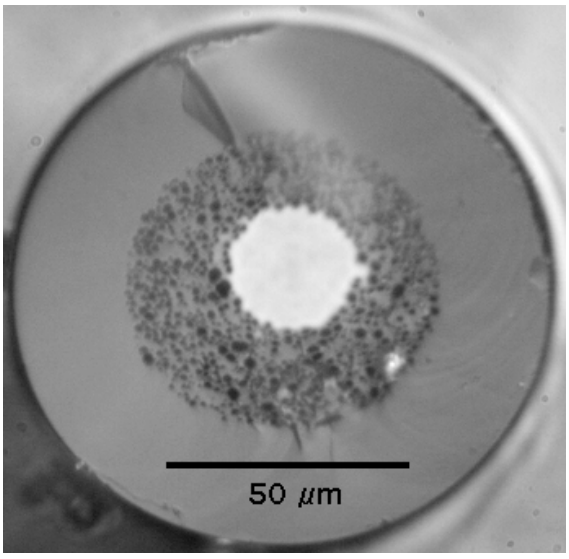

Figure 21: DK 03-01 Optical Micrograph of RHOF Made with Preheated Powder

Fiber was drawn from preform DK 03-01 on two occasions, yielding the fibers labeled spool A and spool B. Although the fiber from spool B was judged to be slightly superior (visual inspection showed spool B to have a moderately higher volume of air) both generated the characteristic smaller and more numerous holes (Figure 22). This indicates that it was the preoxidation of the silicon nitride which is responsible for the altered hole structure, rather than a peculiarity of the draw parameters.

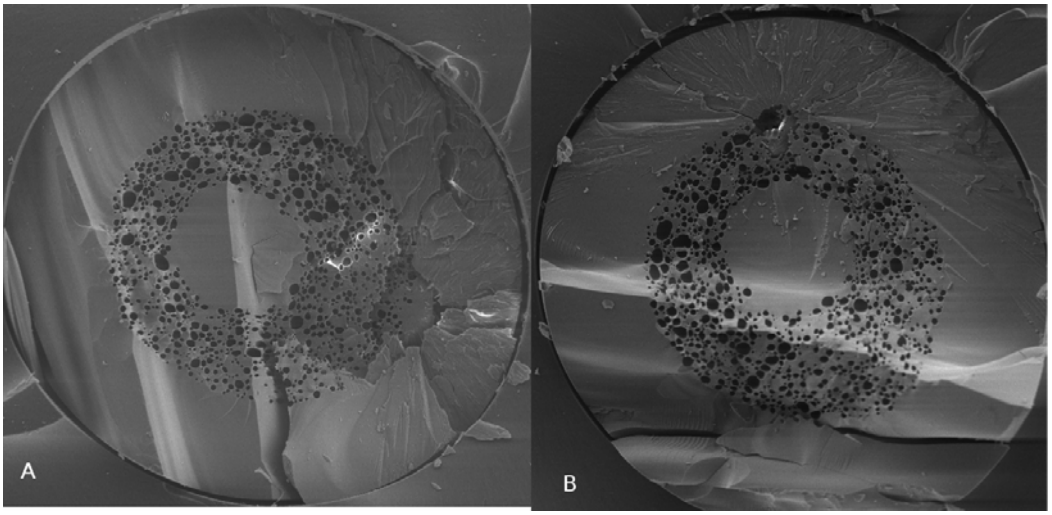

Figure 22: Scanning Electron Micrographs of Fiber From Preform DK 03-01, Spools A & B

Using Vacuum to Prepare Preforms

All vacuum work described in this section was done with a mechanical roughing pump. Actual values of pressure were not available, but are thought to be a very low grade vacuum (more than ten millibar). After initial preforms exhibited problems due to apparent excess air trapping, attempts were made to reduce the amount of air within the preforms by means of pulling a vacuum on the preform before drawing. A schematic of the system used to apply vacuums to the preforms can be seen in Figure 23.

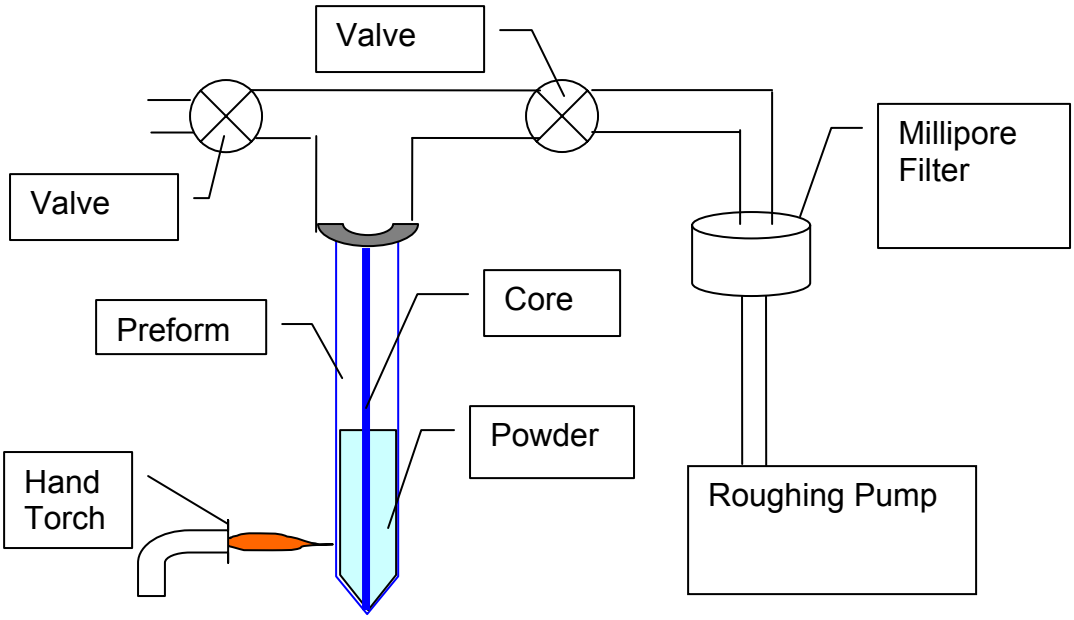

Figure 23: Schematic of Vacuum System for Preforms

First, a vacuum was alternately applied and then the preform was exposed to atmosphere in an attempt to more closely pack the particles. During each cycle the preform had to be tapped to encourage the powder to settle down in the tube. An ultrasonic cleaner was tried to see if it would help settle the powder more easily than the manual tapping; however, it produced no visually discernable effect, whereas during tapping the powder could be seen to be settling. After this process was completed the preforms were left open to atmosphere. Although the air pressure would equalize at standard pressure, the idea was that the volume of the air spaces would be reduced by obtaining a closer packing of the powder. The process did not seem to be effective as it was not possible to draw preform DK02-03 successfully. In this instance there was too much trapped air, resulting in blowouts and severe core migration. With additional information it was realized that the powder mixture of DK 02-03 was excessively high in a gas

producing agent (1% silicon carbide), assuring that the failures observed would have occurred independent of the efficacy of the vacuum system for packing.

Following these initial attempts were made to try to generate two preforms which maintained an internal pressure lower than atmospheric. This was attempted by placing pieces of Pyrex glass on top of the powder before applying the vacuum. The vacuum was applied alternately with tapping on the preform, and the powder was allowed to settle, as in the earlier cases. While keeping the vacuum in place, the preform was heated with a hand torch, from bottom to top, several times, again tapping the preform to settle the powder, as the thermal expansion of the gas forced gaps to form. After this I heated the preform from the bottom up, and then heated the Pyrex, allowing it to melt and form a cap on top of the silica powder, sealing the lower portions of the preform. It was found that it is necessary to preheat the top of the preform tube in order to prevent the vacuum pump from extracting all of the powder. The preheating causes the upper regions to taper down, thereby forming a sort of filter over the top of the powder, reducing the likelihood of the powder being pulled from the preform. After the initial vacuum is drawn on the preform and the powder had settled back down, I applied heat from the hand torch, starting at the bottom and working my way up. As the residual air heated and expanded, the air spaces reopened. Again tapping of the preform allowed the powder to settle back down. Once I reached the upper portions of the powder, I returned the heat to the bottom of the preform and repeated the process. Once the powder had settled again (after two or three

cycles of heating from bottom to top), the torch was applied to the region at the top of the preform where the Pyrex pieces were located. Because the Pyrex melts at a much lower temperature than the silica, it became molten and formed a barrier on top of the powder. Although the Pyrex cracked somewhat during the cooling process, the top was sealed off, thereby keeping the entire powder region of the preform at vacuum.

Upon testing with a hand torch, one of these preforms (DK 02-04) appears to have had a sufficient amount of air removed from it during the vacuum process. This was determined by noting that the preform did not exhibit any blowouts when the hand torch heated the preform to the point where the silica softened. This is the preform which was comprised of 325-mesh silica, with no gas producing agent. Although enough air was removed to prevent blow outs of the preform, there was still too much air to allow for a successful fiber, evinced by the large holes which are present (Figure 24). It is also important to note that the vacuum method is not likely to be highly repeatable, due to the mechanical tapping, as well as the likelihood that the heat applied to the powder will differ between samples. Due to the lack of repeatability inherent in this technique this method is considered to be a poor choice for avoiding the blowouts caused by excessive air trapping.

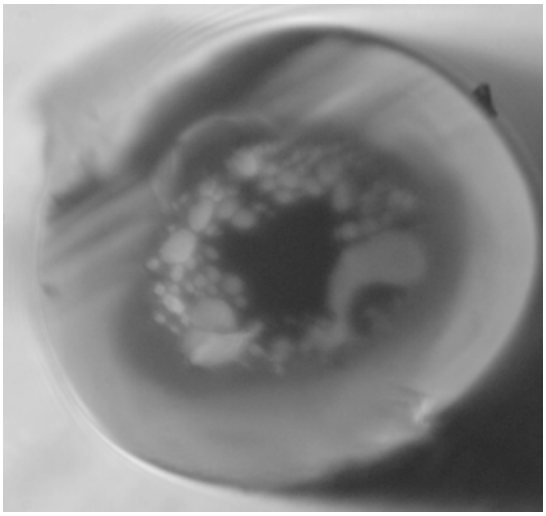

Figure 24: DK 02-04 Optical Micrograph of Fiber from 325-mesh Preform Sealed at Vacuum

One way to avoid the necessity of dealing with excessive air trapping entirely is to use a larger initial particle size, as was the case in the early preforms where the powder was generated by crushing bulk fused silica. When the silica powder which forms the basis of the cladding was changed to a 100-mesh particle size, the issue of excessive air trapping became moot. The larger particles were able to be packed much more readily by simply tapping the bottom of the preform. During draw, any excessive amounts of gas appear to have been able to readily self vent. As a result, relatively precise control of the amount of gas which is contained within the preform becomes possible, since the only significant source of gas is the added fining material, which is trapped due to the sintering of silica powder above it.

Impact of Tube Thickness on Powder Preforms

Preforms have been fabricated using containment tubes of varying thickness. These tubes ranged in size from 6x12 mm up to 19x25 mm. (All tube sizes are designated by the notation of "inside diameter x outside diameter," measured in millimeters.) Most of the tubes that were used have walls that are three millimeters thick. Some powder preforms were fabricated with tubes which were 14x16, mostly with large diameter cores, as would be used for double clad fibers. In general, the preforms with thinner walled tubes have been incapable of establishing a successful draw. I attribute this to the need for a greater amount of structural supporting material than is provided by the thin walls. When a preform with a thin walled outside tube is heated in the furnace, it tends to take a long time to bait off, but once the bait has occurred, the fiber tapers very rapidly, resulting in breakage. In some instances it was possible to establish a fiber draw from a preform which used a 2 mm wall thickness. The most successful draws, however, have been with a preform whose outside tube had an inside diameter of 9 mm and an outside diameter of 15 mm.

Some preforms were attempted with much larger diameter tubes, though still using the 3 mm wall thickness. These preforms were made with both 13x19 tubes and with 19x25 tubes. It was not possible to establish any successful draw from a preform which used a 19x25 tube (DK 02-17). The cause of the failure in this case is not known; however, the mechanism of failure was extreme fragility of the fiber.

Three preforms were fabricated using a 13x19 tube (DK 02-18, DK 02-19, and DK 02-21). While the latter two were able to be drawn into fiber, the fiber was unusable due to their microstructures. The first of these two, DK 02-19, was made with 0.05% silicon nitride (Figure 25). The second which produced any fiber at all was DK 02-21, an image of which can be found in Figure 26. This preform used a 0.074% silicon nitride composition, nearly the same as that used in the successful draw of DK 02-15.

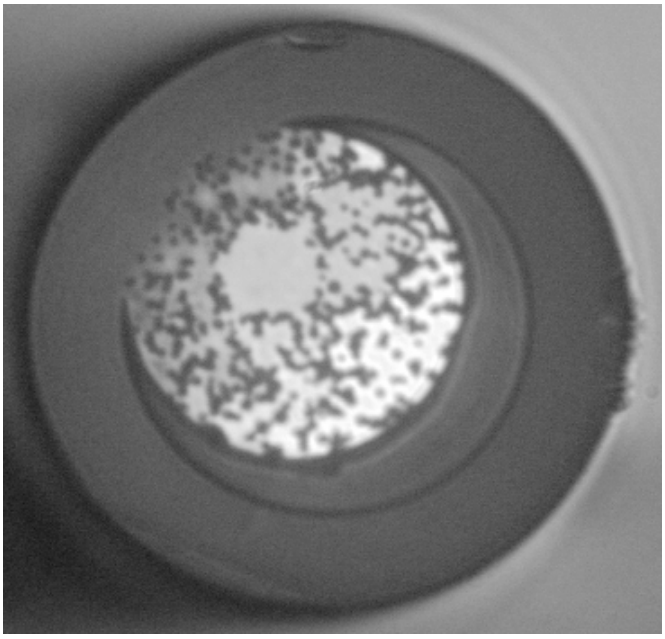

Figure 25: DK 02-19 RHOF Made with 13x19 Tube

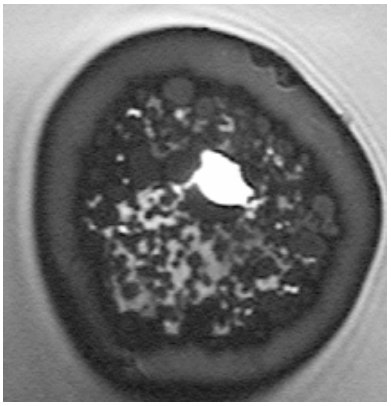

Figure 26: DK 02-21 RHOF Made with a 13x19 Tube

From comparison of the fibers from DK 02-19 and DK 02-21 and from consideration of fibers which were made with smaller tubes, a few conclusions can be drawn. Although the amount of silicon nitride in preform DK 02-21 is the same as in many smaller preforms which generated high quality fiber, this preform did not generate useful fiber (see Figure 26). This may be due to an increase in the amount of trapped gasses, as opposed to the amount of gas generated. The overall fiber has also been significantly distorted from its initial circular geometry. This indicates that the relative amount of the preform which provides structural strength, in this case the outer tube, is insufficient. Despite the fact that the outside tube wall is the same three mm which was successfully used in smaller preforms, this represents a smaller proportion of the structure in the preforms made with larger tubes. Thus when the fibers are drawn to the same 125 μm diameter, there is less overall strength.

In the case of DK 02-19, made with a lesser amount of silicon nitride, the overall structure of the fiber is correct, aside from the large crescent shaped distortion of

the hole (see Figure 25). The holes which were generated, however, were too small and not numerous enough for a good optical confinement.

I believe that both of these problems are the result of the higher thermal inertia of the larger preforms. Because the preforms are larger, two factors come into play. First, the preform must be fed into the furnace at a slower rate, thereby exposing each portion of the preform to the high temperatures for a longer period. In addition, the actual temperature of the furnace had to be higher in order for the core of the preform to be hot enough to be workable. As a result the silica powder was fused over a longer portion of the preform during the draw, thereby trapping more of the gasses. At the same time, the silica which formed the cladding was at a higher temperature (and lower viscosity) for a longer duration of time. This allowed the air holes to migrate much further, resulting in fewer holes. This same phenomenon was likely responsible for the occurrence of the large crescent shaped hole found in DK 02-19.

While there may be a means of avoiding these problems associated with the larger preforms, further work was restricted to systems which use the 9x15 tubes. This was due to early indications of success with this set of tube dimensions. However, this restricts the preform to the use of small core rods when making a fiber with a small core diameter. Since it is generally impractical to use rods smaller than about one millimeter in diameter, this imposes a limit on the minimum core/fiber diameter ratio which can be obtained.

Despite the glass content of the powder, it does not appear to add appreciable strength to the finished fiber. As a result, the final fiber's structure is almost entirely supported by the tube which forms the outer wall. In addition, preforms which are fabricated with a thin walled tube contain a much higher relative fraction of air. When heated in the draw tower, the expansion of this air can lead to excessive swelling of the overall outside dimension of the preform, thereby causing holes in the preform's outer wall.

Impact of Grain Size in Powder Preforms

Preforms were made with glass particles of varying sizes. As a result of the different sizes, the draw characteristics of the preforms can change. In general, the smaller the particle size the more tightly confined the gasses will be within the preform. We have drawn preforms which contain glass powder in sizes ranging from 325-mesh (meaning powder that can fit through the holes in a screen which contains 325 lines per inch, approximately the same consistency as flour) up through powder which averaged particle diameters of about 5 millimeters.

Further work was carried out with a coarser powder. This powder was purchased from Strem Chemicals, Inc. This is a silica powder which has been strained to a 100-mesh size. The powder does, unfortunately, have a lower purity (99.7% pure) than the available 325-mesh powder whose purity can exceed 99.995%. As a result of the lower purity, the fibers fabricated are likely

to be subject to the enhanced optical loss arising from material absorption. An ideal approach is to use a high purity (perhaps synthetic) silica, and to grind and sift it to achieve the desired particle size. In the interest of expediency, however, the commercial powder from Strem was used.

Two effects from an increase in particle size are: 1) to allow for easier paths for the air to escape and, 2) to reduce the amount of surface area of the powder, thereby lowering the amount of adsorbed gasses which are present in the preform initially. When the preform is heated in the furnace, the gasses which are liberated should escape from the preform. As the temperature rises high enough to start the process of fusing the powder, the fining material will oxidize, releasing additional gas into the now semi-sealed region to provide the porosity of the fiber.

Preforms which were fabricated from this material, including DK 02-05 and DK 02-07, did not experience the extreme expansion demonstrated in the earlier preforms, fabricated from a finer powder. One preform fabricated using this powder which did experience a blow out was DK 02-06, a thin walled, large core fiber. In this case, the failure appears to be due to the minimal strength of the exterior wall.

References:

[1] J.C. Knight, T.A. Birks, P.St.J. Russell, D.M. Atkin, "All-silica single-mode fiber with photonic crystal cladding," Optics Letters **21**, 1547-1549 (1996).

[2] N.M. Litchinitser, A.K. Abeeluck, C. Headley, and B.J. Eggleton, "Antiresonant reflecting photonic crystal optical waveguides," Optics Letters **27**, 1592-94 (2002).
[3] "Large Mode Area Photonic Crystal Fiber Datasheet," http://www.crystal-fibre.com/datasheets/LMA-25.pdf Image is copyrighted by Crystal Fibre A/S
4 Image from "Airguiding Hollow-Core Photonic Bandgap Fibers," http://www.crystal-fibre.com/products/airguide.shtm, Image is copyrighted by Crystal Fibre A/S
[5] S.E. Barkou, J. Broeng, and A. Bjarklev, "Silica-air photonic crystal fiber design that permits waveguiding by a true photonic bandgap effect," Optics Letters **24**, 46-48 (1999).
[6] Patent: DiGiovanni, et. al. "Article comprising a micro-structured optical fiber and method of making such fiber," Patent Number: 5,802,236 (Sep. 1, 1998).
[7] J.C. Knight, T.A. Birks, R.F. Cregan, P.St.J. Russell, and J.P. de Sandro, "Photonic crystals as optical fibres- physics and applications," Optical Materials **11** 143-151 (1999).
[8] P.St.J. Russell, J.C. Knight, T.A. Birks, R.F. Cregan, and B.J. Mangan, "Photonic Crystal Fibres," ECOC 97.
[9] A.K. Abeeluck, N.M. Litchinitser, C. Headley, and B.J. Eggleton, "Analysis of spectral characteristics of photonic bandgap waveguides," Optics Express **10**, 1320-1333 (2002).
[10] V. Rastogi and K.S. Chiang, "Holey optical fiber with circularly distributed holes analyzed by the radial effective index method," Optics Letters **28**, 2449-51 (2003).
[11] J.K. Ranka, R.S. Windler, A.J. Stentz, "Optical properties of high-delta air silica microstructure optical fibers," Optics Letters **25**, 796-798 (2000).
[12] John Lee Watson Noell, The preparation and characterization of PEK/TEOS glasses by the sol-gel method ,Thesis (M.S.)--Virginia Polytechnic Institute and State University (1987).
[13] Aerogels : proceedings of the first international symposium, Wurzburg, Fed. Rep. of Germany, September 23-25, 1985 / editor, J. Fricke.
[14] Information derived from conversations with Dr. Gary Pickrell, Virginia Tech.
[15] J. Canning, A. Canagasabey, "Hypersensitisation Of Optical Waveguides: Towards Industrial Application," Journal of Microwaves and Optoelectronics, **3**, 113-126 (2004).

Properties of Random Hole Optical Fibers

Loss

There are a number of factors which influence the loss function in random hole optical fibers (RHOF). The most important factors are: the composition of the core and cladding, and the spatial geometry of the holes in the cladding region. Loss per meter curves can be seen for fibers DK 02-15, DK 02-23, and DK 03-01 in Figure 27. While DK 02-15 and DK 02-23 have approximately the same hole structure in the cladding, they use different materials for the core. DK 02-23 uses the high purity synthetic core, whereas DK 02-15 uses a bulk fused quartz rod for the core. Similarly, the core material that is used in DK 03-01 is the same as that used in DK 02-23, but the hole structure is significantly finer. Therefore, this trio of fibers allows us to decouple the loss issues associated with material loss in the core from that of confinement due to hole structure. A summary of these characteristics can be seen in Table 2.

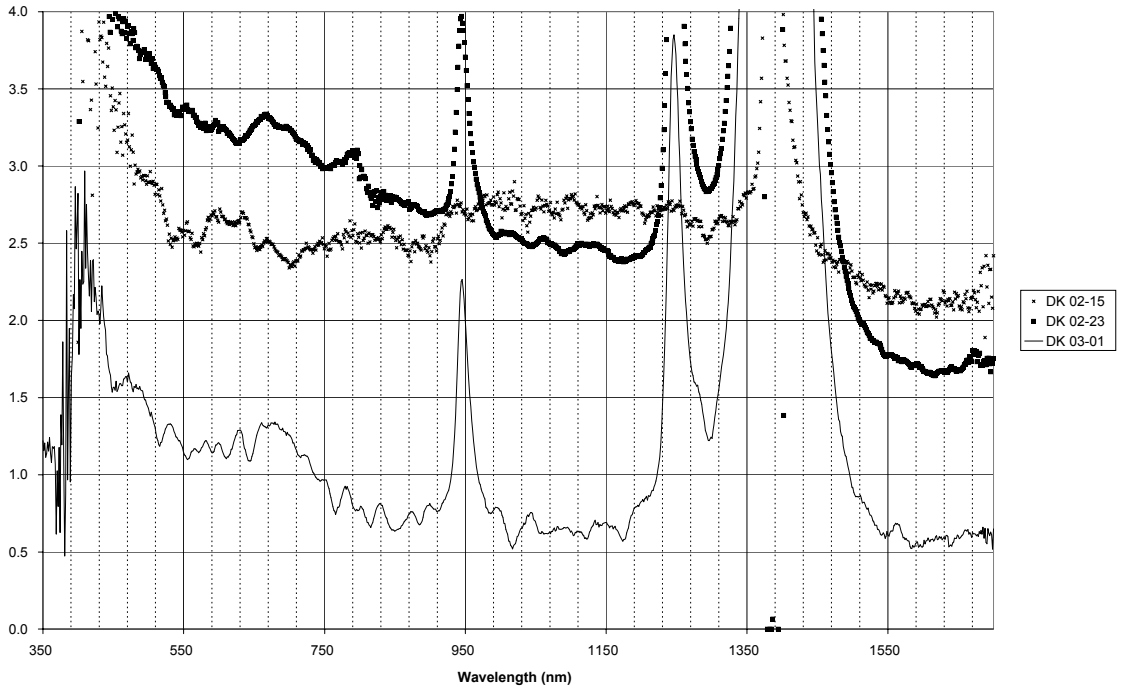

Figure 27: Loss Per Meter of Three Different RHOFs

Table 2: Comparison of Fibers DK 02-15, DK 02-23, and DK 03-01

Preform	Core Material	Hole Structure	Loss at 1550 nm (dB)
DK 02-15	Fused Quartz	Fewer, Larger Holes	2.11
DK 02-23	Synthetic Silica	Fewer, Larger Holes	1.77
DK 03-01	Synthetic Silica	More, Smaller Holes	0.60

The first important distinction is that the loss curves for fibers DK 02-15 and DK 02-23 are quite similar in value across much of the spectrum. This implies that the material losses are relatively minor in this type of fiber, at least in the form that the fibers are currently drawn. As other loss mechanisms are reduced, the relative importance of material loss will increase dramatically. Two vital

differences between these are the flatter loss spectrum of DK 02-15, and the much larger loss peak of DK 02-23 at 1385 nm. The loss peak is due to the much higher OH content of the core material used in DK 02-23 (Saint Gobain Spectrosil 2000).[1]

The difference in loss character between the first two fibers and DK 03-01 is substantial. Since this fiber was fabricated with the same materials as DK 02-23, we can attribute the large reduction in loss exclusively to an improvement in the waveguiding characteristics of the structure. The smaller (and more numerous) holes seem to result in a higher degree of confinement of the optical power. Again, as in the case of DK 02-23, the loss due to the hydroxyl group at 1385 nm is substantial, due to the high OH content of the core. Likewise, the loss peak at approximately 950 nm is also due to the composition of the core material, given its presence only in the cases of fibers DK 03-01 and DK 02-23. This data strongly suggests that by further increasing the number of holes, while reducing the hole diameter, the loss of the fibers could be further reduced.

Dispersion

One of the key parameters of any optical fiber is its dispersion. The dispersion is a measure of the change in refractive index which guided light experiences as a function of wavelength. In general, the dispersion can be separated into contributions from the physical properties of the material (including nonlinear

terms of the dispersion), and the waveguide dispersion (which is a function of the fiber's geometry), which includes modal dispersion.

The first component of the total dispersion is the material dispersion. All materials have an innate dispersion, which is a function of the materials composition.[2] The dispersion is effectively the derivative of the group index as a function of wavelength. The definition of the group index, as a function of wavelength and refractive index (which is itself a function of wavelength), is given in Equation 1.[3]

$$N(\lambda) = n(\lambda) - \lambda \frac{dn}{d\lambda}$$

Equation 1: Definition of Group Index

Here, n is the refractive index of the material, which is a function of the wavelength, λ. Using this definition of group index, the material dispersion of a system can be defined as in Equation 2. There is always a minimum value in the group index; the wavelength at which this occurs is the zero dispersion wavelength. In a silicate system (including germanosilicates) this value is at a wavelength of approximately 1.28 microns.[4]

$$D(\lambda) = \frac{1}{c}\frac{dN}{d\lambda} = -\frac{\lambda}{c}\frac{d^2 n}{d\lambda^2}$$

Equation 2: Definition of Dispersion

Here D is the dispersion, c is the speed of light, and N, n, and λ have the same definitions given above. As previously mentioned, the actual dispersion in a fiber

is a combination of the material dispersion and the waveguide dispersion. The waveguide dispersion, however, can only shift the zero dispersion wavelength to *longer* wavelengths.[4] As a result, dispersion shifted fibers (which have a zero dispersion wavelength of 1.55 microns) as well as dispersion compensating fibers (which have a longer zero dispersion wavelength) can be manufactured. The fiber geometry cannot, however, result in a shorter zero dispersion wavelength than that which is mandated by the material dispersion.[4]

One characteristic of holey fibers is that they can have dispersion properties that are vastly different from conventional fibers.[5] A certain proportion of the light travels in the air holes as an evanescent field. Therefore, the material dispersion of the fiber becomes a weighted average between the silica and the dispersion associated with the gas in the air holes.[5] The precise weighting of this average may be extremely complex, particularly in the case of random hole fibers in which the individual holes may interact with the light differently. An empirical measurement of the dispersion may yield the most accurate means of determining the proportion of optical power guided in silica, as opposed to the air holes. If one chooses to perform an unweighted average to determine the average index, one arrives at a remarkably low cladding index as seen in Table 3. In this instance the reflection micrograph seen in Figure 28 was measured in nine regions. The grayscale micrograph consists of darker regions, which are the air spaces, and lighter regions which are the silica of the fiber. Thus the

intensity count of each pixel can be used to asses whether that pixel contains air or silica.

Five regions were taken at random from within the cladding, three from the core, and one from the air surrounding the outside of the fiber. The average intensity for each of these regions was measured (on a scale of 0 to 255). Assuming a linear relationship between the cross section which is comprised of air and the average intensity of that region, Table 3 shows that the cladding is comprised of nearly 32% air by volume. Applying that percentage to an average index, yields the cladding region having an average index of just over 1.3.

Table 3: Geometrical Analysis of DK 03-01

Sample Number	Area (square Pixels)	Mean Intensity Count	Region	[A value of 0 is a saturated pixel, a value of 255 is a completely dark pixel]	
1	189.655	130.792	(Clad)		
2	205.47	130.911	(Clad)		
3	206.421	123.293	(Clad)	Average Cladding Value:	I_{cl}=128.0348
4	168.847	124.014	(Clad)		
5	185.969	131.164	(Clad)		
6	103.924	95.616	(Core)		
7	74.911	93.932	(Core)		
8	60.642	94.618	(Core)	Average Core Value:	I_{co}=94.722
9	133.413	199.06	(Air)	Air Value:	I_{air}=199.06

$$\%Air = \frac{I_{cl} - I_{co}}{I_{air} - I_{co}} = 31.93\%$$

Average Index=

$$\%Air * n_{air} + (1 - \%Air) * n_{SiO_2} = 1.306325021$$

As the size of the air holes in a holey fiber decreases (particularly in the case of a random hole fiber), one can more readily model the behavior of the fiber as a

step index structure. In the case of ordered hole fibers, a more accurate approach than modeling with a single step geometry is to treat the fiber as a series of rings, each with it's own average index.

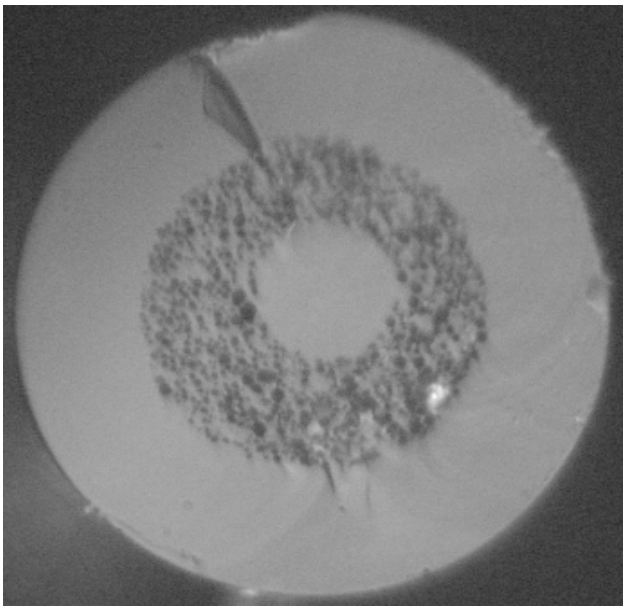

Figure 28: Optical Micrograph of DK 03-01 Used for Geometrical Analysis (Reflection Illumination Only)

Modal Structure

One of the characteristics which is most heavily emphasized in the study of photonic crystal fibers and ordered hole fibers is their unusual mode properties. Early research of holey fibers determined that these fibers supported far fewer modes than one would find in conventional fibers with comparable core diameters.[6] It has been found that these fibers are capable of being single mode at any wavelength which the material can transmit.[7] Measured fibers have shown single mode guidance over a range from 458 nm out to near 1.55 microns.[8] Originally, these modal properties were attributed to the photonic

bandgap nature of photonic crystal fibers. It later became clear that holey fibers which did not have the structure necessary for photonic bandgap effects were also capable of producing an expanded single mode range.[9]

The reason why the extended single mode behavior can be seen in holey fibers (as opposed to photonic crystal fibers) is caused by the fact that they are fundamentally leaky structures.[9,10] The higher order modes are more poorly confined in a microstructure fiber, leading to a significantly higher attenuation. As a result, after a short propagation distance, the fiber appears to be single mode.[11]

The random hole optical fiber also demonstrates this characteristic. A pseudo-color photograph of the far field pattern generated by fiber from DK 03-01 can be seen in Figure 29. The fiber was pressed against a rough surface a short distance from the launch point to ensure that all available modes were excited. This was done by placing the fiber between two pieces of aluminum which had been heavily scored by drills, saws, etc. These surfaces were rough on both a macroscopic and microscopic scale, although there was no uniformity to the surface variations. The fiber was then left loose for approximately two meters, and the output face was projected on a screen. The fact that the nodes (the dark areas within the pattern) are visible indicates that this fiber is guiding less than 10 modes.[12] Were this fiber to support a significantly higher number of modes the dark regions in this modal patter would be washed out, resulting in the characteristic speckle pattern of multimode fiber. Note that a conventional fiber

(with $\Delta n = 0.005$) which has a core diameter of 26 microns would support several thousand modes at this wavelength. Were this calculation to be applied to a strict average index value of the cladding which was shown in the previous section to yield a $\Delta n \approx 0.15$ it would be far higher. Thus, while the RHOF has not been proven to be capable of the enhanced single mode performance, it has certainly demonstrated that it exhibits a vastly reduced mode number, and it seems likely that it would demonstrate the single mode behavior if the core diameter were reduced a little further.

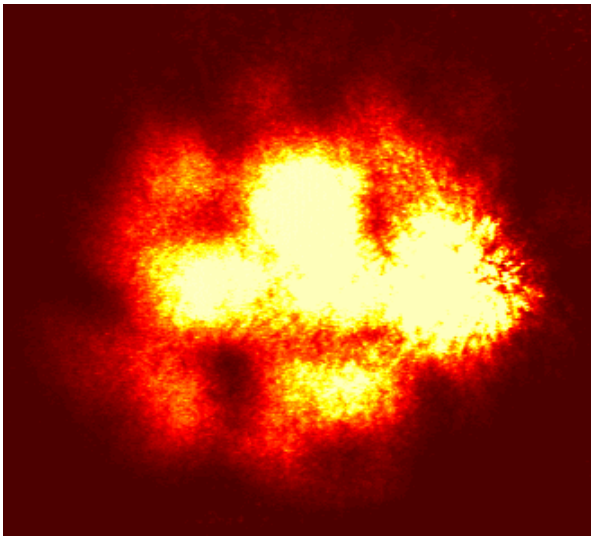

Figure 29: Far Field Mode Pattern Generated by 633 nm Light in Fiber DK 03-01

Pressure Sensitivity

One of the unusual characteristics of the random hole optical fibers is their innate pressure sensitivity. When pressure is applied to the fiber, in either linear compression or hydrostatically, a wavelength dependent loss occurs in the fiber.

Three of the fibers which were tested for pressure sensitive loss are DK 02-15, DK 02-23, and DK 03-01. These fibers were chosen because of their low baseline loss and because they spanned the range of core material and hole size.

While many fibers are sensitive to pressure, either in their 'as drawn' state, or due to a process which has been applied to them (such as writing a Bragg grating)[13] nearly all mechanisms which yield a pressure sensitivity in a fiber system are similarly susceptible to temperature variation. As a result, there are very few fiber systems that can be used to measure either pressure or temperature, without independent measure of the other parameter.[14] The primary reason for this correlation is due to the various mechanisms by which the two sensitivities are measured. In most cases these parameters are measured by detecting a change in the linear extent of the fiber, in one dimension. One example is a tension measurement made using the stretching of a fiber containing a Bragg grating.[15] Due to the coefficient of thermal expansion, however, a change in the temperature of the fiber also results in a similar change in the period of the Bragg grating. Therefore, when one measures a wavelength shift in the peak reflectivity of a Bragg grating, it could be due to either a tension applied to the fiber, or an increase in the fiber's temperature at the grating's location.

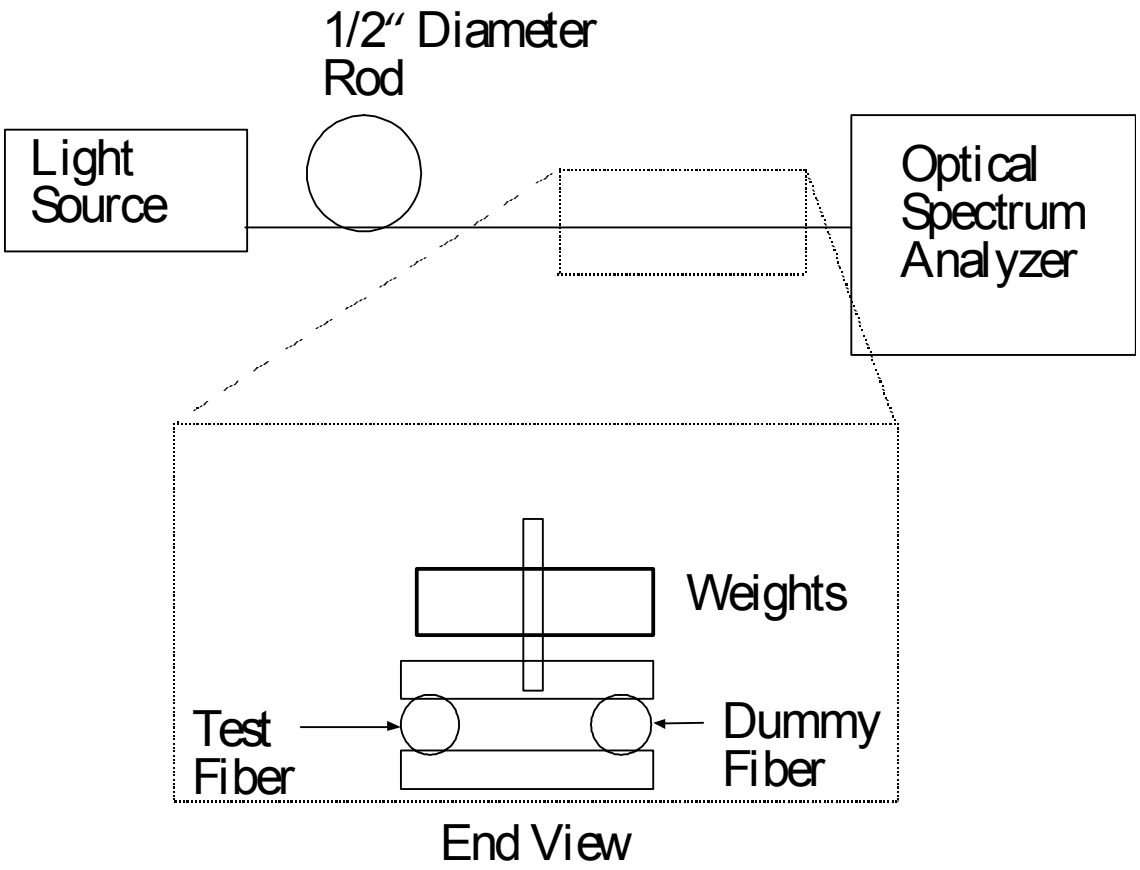

Figure 30: Schematic of Pressure Sensing Test

One of the unique characteristics of the random hole optical fibers is that it exhibits a pressure sensitivity *without* the same dependence on temperature. A schematic of the layout used to make the pressure sensitivity measurements can be seen in Figure 30. To take the measurements, white light was coupled into the fiber from a tungsten bulb. The fiber was then wrapped around a half inch post in order to strip any high order, unstable modes. The fiber then passed under one end of a metal plate 1.125 inches wide. Under the other end of the fiber was a second piece of fiber, ensuring that the metal plate distributed the weight evenly. A series of weights were then placed on the metal plate, and the

transmission spectrum was measured for each weight, and subtracted from a baseline taken with just the metal plate. In Figure 31 the pressure sensitivity curves for one of the RHOFs (DK 03-01) can be seen. The masses which were applied to the fiber were, in units of grams: 100, 300, 500, 800, 900, 2000, 3000, and 4000. Finally, after all of these measurements, all the masses were taken off and the measurement was made again, with just the metal plate back in place, to check for any hysteresis. This is the curve labeled '0' g.

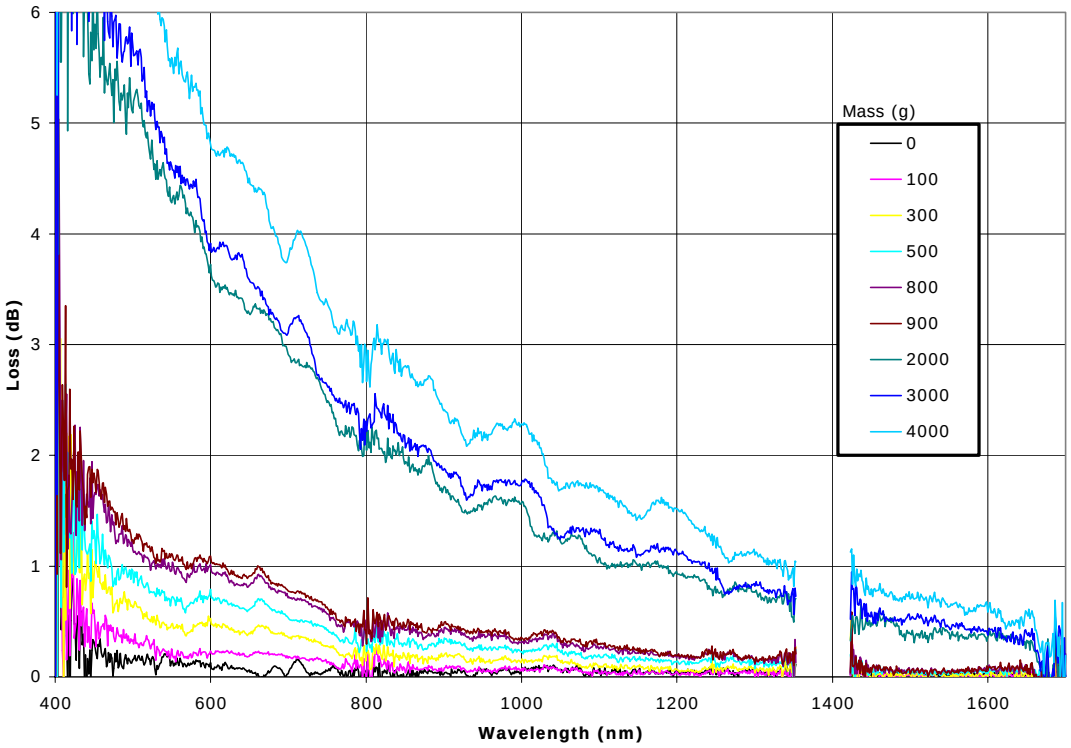

Figure 31: Pressure Sensitivity of DK 03-01

The first item of note

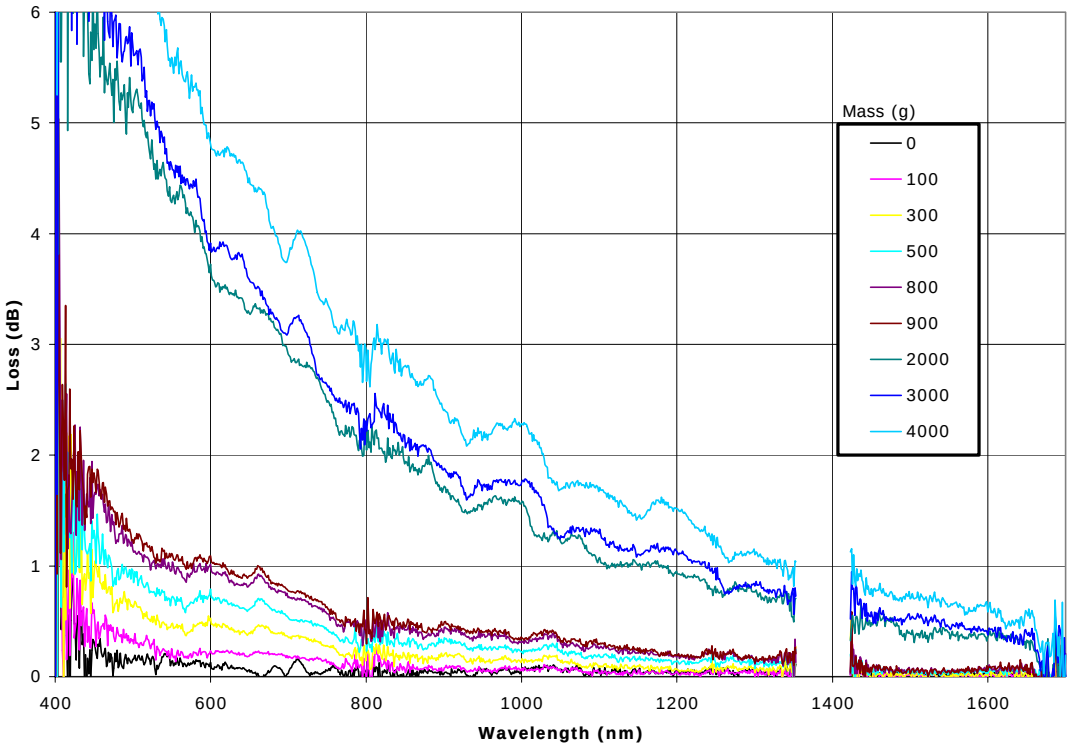

is that the losses are much higher at the shorter wavelengths and then decrease substantially through the longer wavelengths. There is a region surrounding 1385 nm where this data is not available because the background loss due to the hydroxyl ions is so large that a reliable baseline could not be established. As previously mentioned, the high concentration of hydroxyl ions in fiber DK 03-01 is due to the use of synthetic silica for the core material. A similar issue occurs at the very shortest wavelengths (those with wavelengths shorter than approximately 450 nm). In this case the intrinsic loss of the fiber is high enough that the pressure sensitivity data becomes quite noisy.

Also seen in Figure 30 is that the loss increases monotonically with pressure. This can also be seen in Figure 32, which shows the loss as a function of applied

mass, for a series of different wavelengths. There are some outlying points at 2 kg mass, but other than that, the curves are all quite linear. In the case of the curve for the 600 nm data, disregarding the 2 kg data point, the data can be fit linearly with an R-squared value of 0.997. The R-squared value can be between zero and one, with a value of one indicating a perfect match between the data and trend line.* For use in sensing applications, the linearity of this response is particularly valuable. While a nonlinear response can be accounted for by processing the data, it is vastly preferable to have linear data, which can generally yield much more reliable measurements.

---

* R-squared (also called the coefficient of determination) is defined by: $R^2 = \frac{\sum\left(\hat{Y}_i - \bar{Y}\right)^2}{\sum\left(Y_i - \bar{Y}\right)^2}$ where $\hat{Y}_i$ is the value of the curve fit at each data point, $\bar{Y}$ is the average value of all data, and Y_i is the value of each data point.

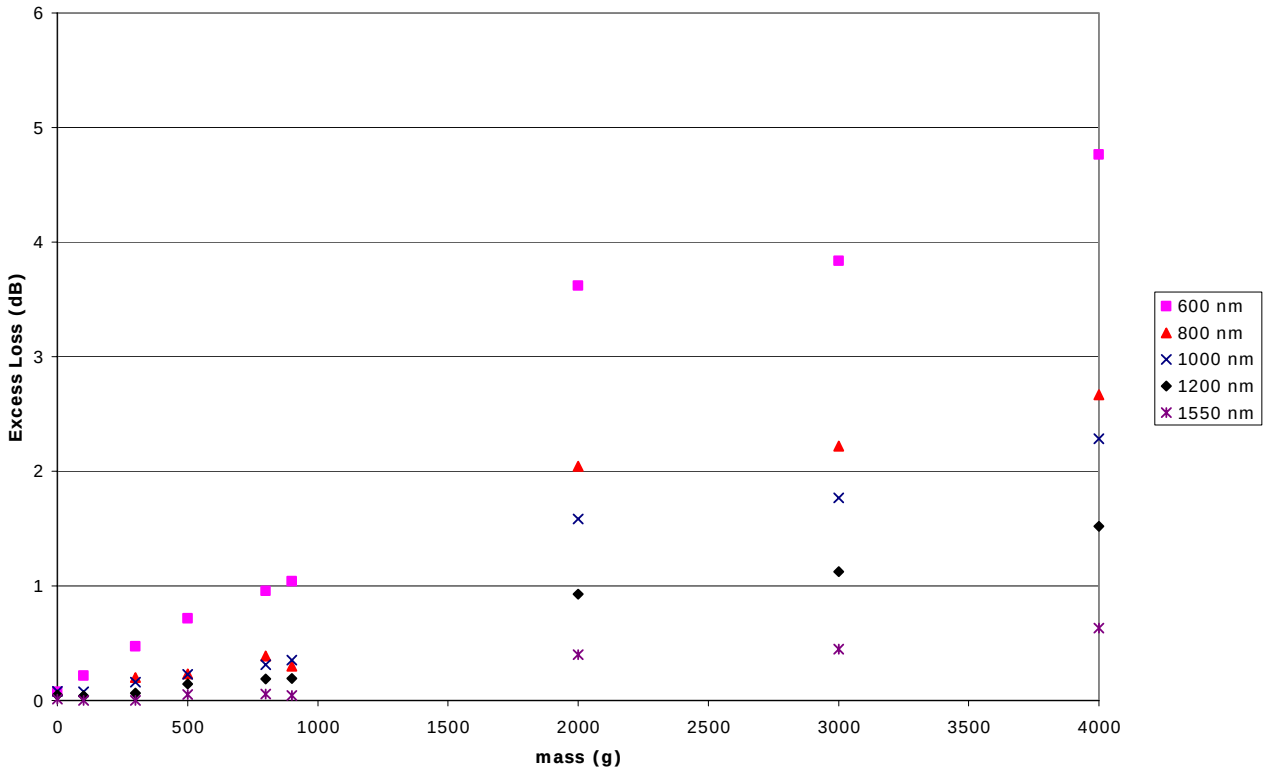

Figure 32: Loss Versus Weight Curves for DK 03-01 at Selected Wavelengths

Experiments were conducted to determine if pressure sensitivity was a universal property of all holey fibers. In order to investigate this theory, an ordered hole optical fiber (IT 03-06) was tested in the same fashion as DK 03-01. An optical micrograph of the fiber used in this trial can be seen in Figure 33. The mass of the applied weight used in this test was 2 kg. Any spectrally dependent loss which was induced by the application of pressure was below the level of noise of the measurement.

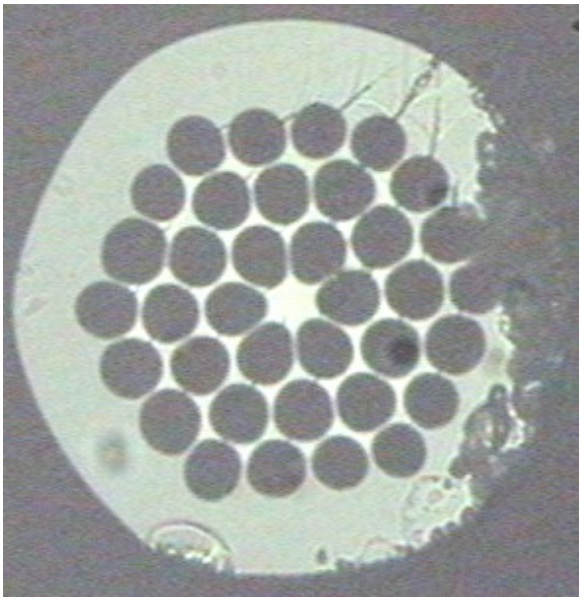

Figure 33: Optical Micrograph of Ordered Hole Fiber (IT 03-06)

We also checked fibers DK 02-15 and DK 02-23 to verify that the pressure sensitivity is not a characteristic which is unique to fiber DK 03-01. Both of these fibers showed similar pressure sensitivity. A plot of the data for DK 02-15 can be seen in Figure 34, and that of DK 02-23 can be seen in Figure 35. In the case of DK 02-15 weight 1 has a mass of approximately 400 grams and weight 2 has a mass of 500 grams. In this case, weight 1 is also acting as the pressure distributor, spreading the mass over a length of 4.95 cm. Weight 1 also acted as the only means of distributing the pressure on the fiber, thereby rendering the precise pressure values inaccurate. The general trend of the data is clear, however. As the mass is increased, there is an increase in loss at the shorter wavelengths. At the longer wavelengths, those above 1200 nm, there is generally very little difference in the loss as a function of pressure.

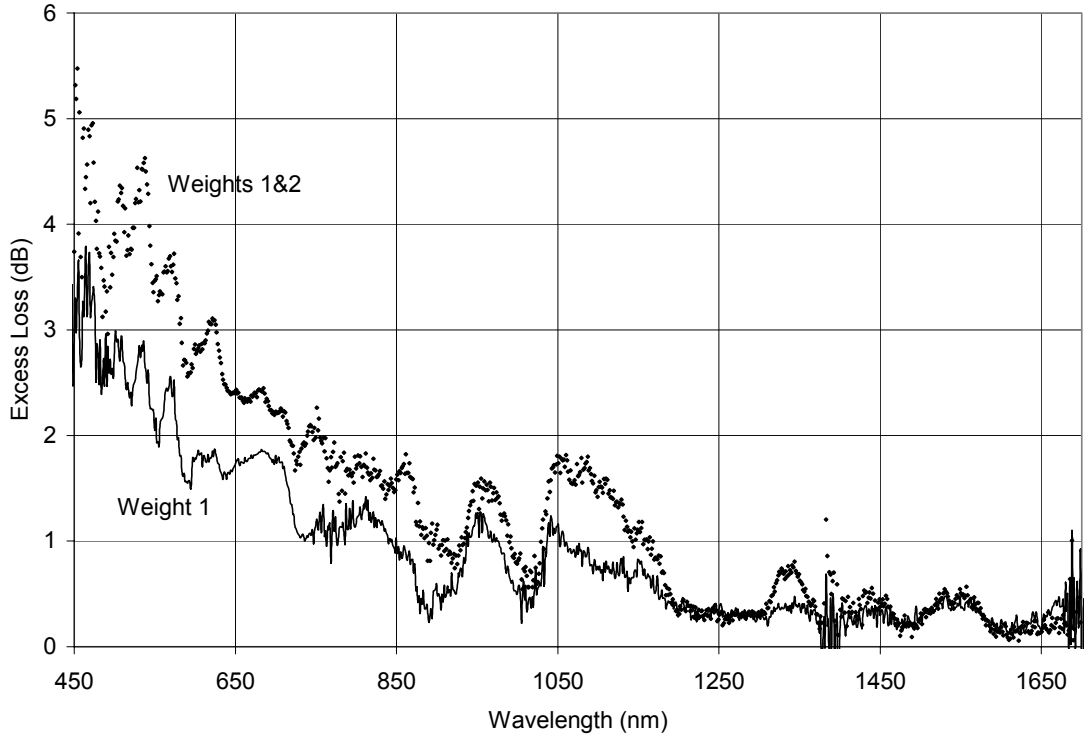

Figure 34: Pressure Sensitivity of Fiber DK 02-15

The pressure sensitivity of fiber DK 02-23 can be seen in Figure 35. As in the case of fiber DK 02-15, the weight was distributed along a length of 4.95 cm. In this case, however, the baseline was provided by the weight of this block, and was subsequently subtracted from the later data. After that, a mass of 300 grams and a mass of 500 grams were set on top of this block, and additional spectra were acquired.

There are several anomalies in this plot (Figure 35) that are noteworthy. Although the data still shows that the pressure sensitive loss is present, and that the loss is increased at the shorter wavelengths rather than the longer wavelengths, it does not drop off to zero loss in the long wavelength region.

Furthermore, the curves cross in several locations. It is unclear whether this is an artifact of the measurement, or if, for some reason this fiber does not exhibit the same linearity of response as the others.

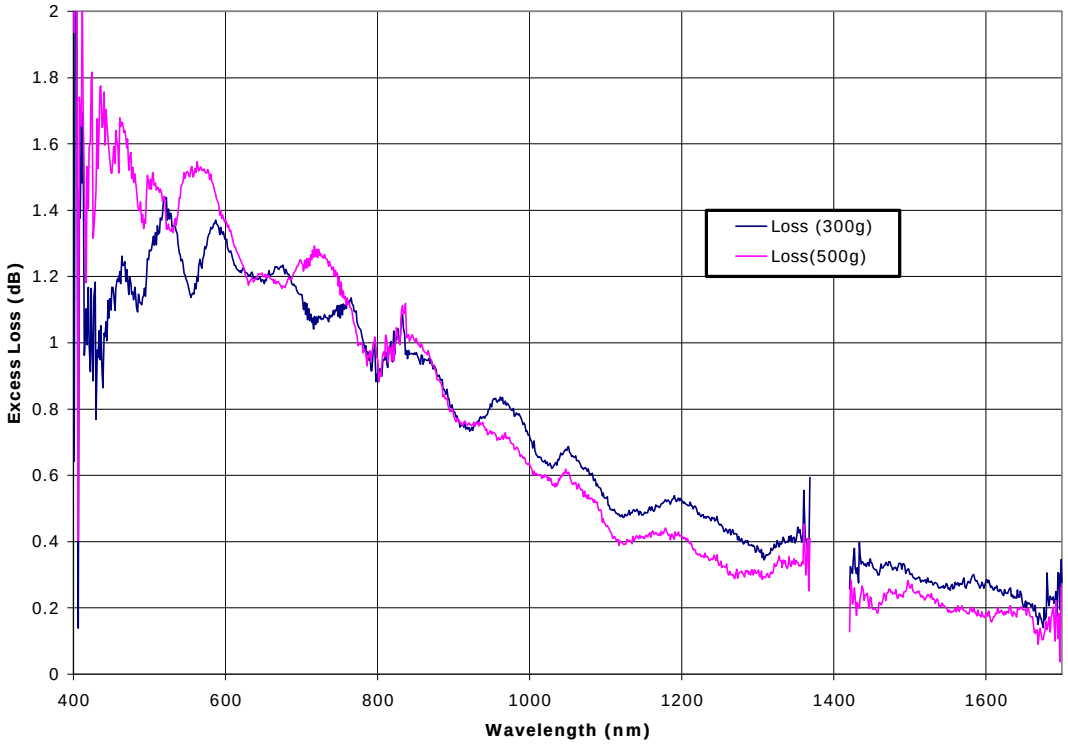

Figure 35: Pressure Sensitivity of Fiber DK 02-23

In addition to the pressure sensitivity which is caused when a mass is placed on top of the fiber, the fiber also exhibits sensitivity to hydrostatic pressure. Fiber DK 02-23 was tested in a pressure gauge calibration system, which was made by Applied Pressure Products. A twelve inch length of the fiber was passed through a stainless steel tube which was pressurized with fluid. The data from this test can be seen in Figure 36, and show the loss values which occurred at 683 nm.

Each of these data points was obtained by subtracting the baseline data point at 14 psi from the power reading for the given pressure.

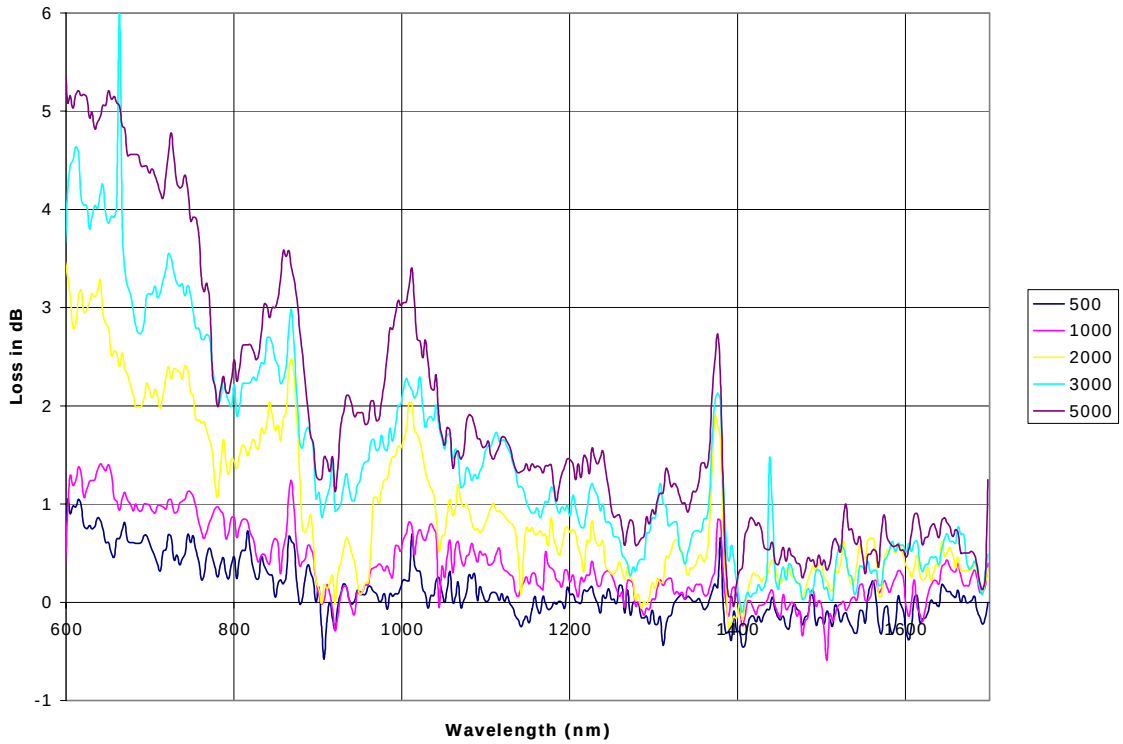

Figure 36:Pressure Sensitivity to Hydrostatic Pressure in Fiber DK 02-23

As in the earlier measurements of pressure sensitivity there are a few things which are immediately apparent. The pressure sensitivity is still present under hydrostatic measurement. As before, the loss at shorter wavelengths is much greater than that at longer wavelengths. Unfortunately, the hydrostatic data is artificially noisy due to a need to redigitize the data from hard copy.

Figure 37 is a plot of the same hydrostatic information base, separated out by wavelength. This helps determine whether the pressure sensitivity of the fiber is linear. In Figure 37 there is also a linear curve fit to the data from the 600 nm samples. Again, although this data is noisy, it does demonstrate that the pressure sensitivity carries over into the hydrostatic realm and that it appears to be linear (with an R^2 value of 0.96).

One consideration regarding this data is that it was taken from fiber DK 02-23 which has not exhibited the same degree of pressure sensitivity as the later fiber DK 03-01. Despite this, the demonstration of principle indicates that the mechanism of pressure sensitive loss needs to account for both linear and isotropic pressure.

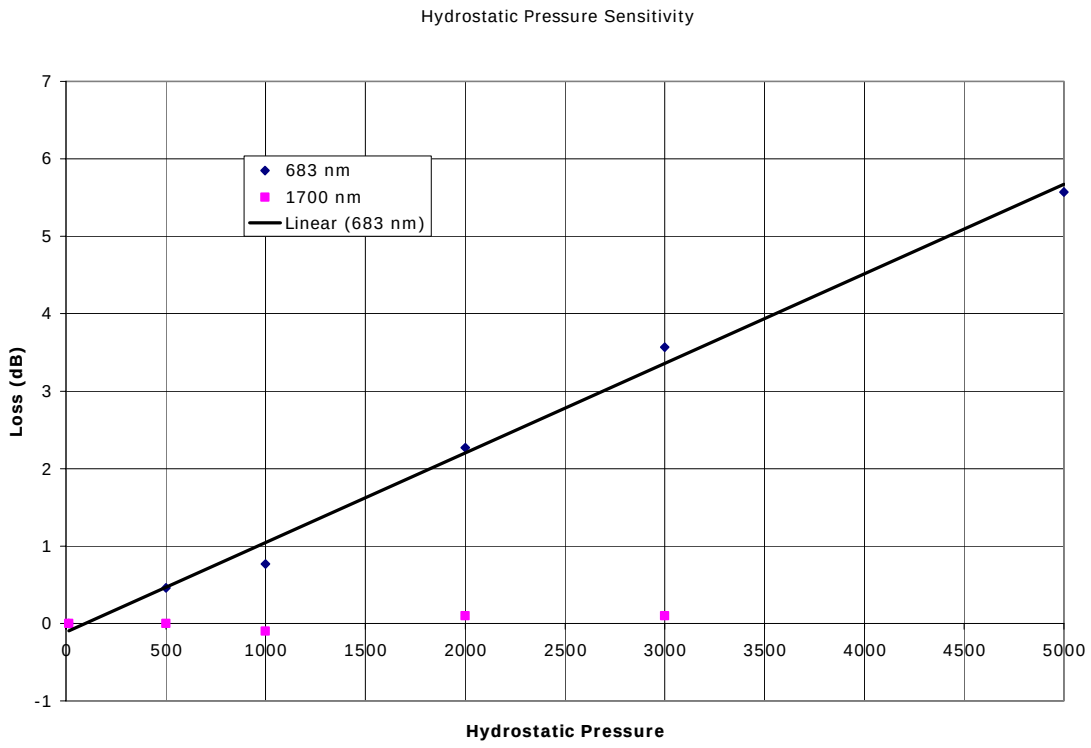

Figure 37: Hydrostatic Pressure Sensitivity of Fiber DK 02-23 Broken Down by Wavelength

Figure 37 also shows data that was taken simultaneously at a wavelength of 1700 nm. While the available data for the hydrostatic tests is minimal, it does show that the fiber exhibits its unusual sensing characteristic in a system where the pressure is applied nearly isotropically.

There are several possible causes of the pressure sensitivity exhibited in RHOFs. The most probable cause is that the pressure acts as a mode scrambling mechanism. The application of pressure will create a small displacement of the portion of the fiber that is under pressure, resulting in a distortion of the core cladding interface. This distortion provides the impetus for light to be coupled between the various modes. As noted previously, the

reduced mode behavior of microstructure fibers is ascribed to the imperfect confinement of the modes (often termed “leaky modes”.) The separation of mode angles in a multi-mode fiber is given by: $\Delta\theta = \lambda/4an_1$, where a is the core radius and n_1 its index.[16] Due to the presence of the wavelength in the numerator the angular separation between modes will be diminished for the shorter wavelengths. This is further compounded by the fact that the refractive index of silica is higher for shorter wavelengths (discounting the anomalous index in the vicinity of an absorption line).[17] Thus, when the fiber is perturbed by the application of pressure, the shorter wavelengths will be subject to a significantly higher level of mode scrambling. The resultant evolution of the power distribution is described by[18]:

$$\frac{\partial P(\theta, z)}{\partial z} = -A\theta^2 P + \frac{D}{\theta}\frac{\partial}{\partial\theta}\left(\theta\frac{\partial P}{\partial\theta}\right)$$

Equation 3: Power Evolution as a function of angle and distance due to intermodal coupling

where:

$P(\theta, z)$	=	the angular power distribution as a function of mode angle and distance;
D	=	$d_0\left(\lambda/4an\right)^2$ [d_0 is the zero order term of the coupling coefficient];
λ	=	free space wavelength;
a,n	=	core radius and refractive index;
A	=	Second order coefficient in the expansion of the loss due to scattering and absorption as a function of angle (i.e. $\alpha(\theta) = \alpha_0 + A\theta^2 + \ldots$)

Noticing that the term D here is a function of the square of the mode separation angle, one readily finds the source of the wavelength dependence of the pressure sensitivity in RHOF.

Due to the relatively high attenuation of the RHOFs previously indicated, the light which has been coupled into higher order modes is rapidly attenuated. The implication of this is that while the mode scrambling process is symmetrical (there is an equal probability of scrambling in either direction between two given modes) there is little to no power in the high order modes to be scrambled into a low order mode. This attenuation will continue well beyond the region of the mode scrambling, resulting ultimately in a near total extinction of the scrambled modes. As a result, the application of pressure results in an extinction of optical power rather than a redistribution of power which would occur in a fiber with lower loss. In effect, this mechanism is a variety of microbend loss, although it is likely enhanced due to the microstructured fiber's propensity for scattering loss at the core-cladding interface.

Another possible source of the pressure sensitive loss is through a mechanism equivalent to quantum tunneling. If the holey fibers' modes are only marginally confined under the unstressed condition, the addition of pressure may sufficiently deform the hole structure close to the core sufficiently to allow the evanescent fields to couple into the small silicate spaces within the pore band. One way to

consider this is by looking at the depth of the evanescent field from a wave striking a core-cladding interface. The depth of the evanescent field is given by[3]:

$$d = \frac{\lambda}{2\pi\sqrt{n_{co}^2 Sin^2(\theta_i) - n_{cl}^2}}$$

Equation 4: Depth of evanescent field at core-cladding boundary

where θ_i is the angle of incidence of the field striking the interface. Because the evanescent coupling from region A to region B is a function of the overlap of the electric field from region A with the index of region B, the closer these two regions are to each other the stronger the coupling will become. Thus, as the external pressure compresses the pore band it will bring more of the filaments of silica from the pore band within the evanescent field from the core, enhancing coupling.

Since the light cannot be guided over a significant distance in the pore band (due to the variations in the physical structure there) this light would then be scattered out of the fiber and be observed as loss. This mechanism would apply equally in both the linear and hydrostatic compressive cases. If this model of the loss is accurate, it indicates that in the extreme case of many very small holes (when the holes and solid silicate regions within the pore band are significantly smaller than the wavelength of the light) the pressure sensitive loss would be diminished, since there would not be a suitable region for the light to tunnel into.

An alternate explanation is that the pressure is inducing a birefringence, and thereby changing the modes which can be supported by the fiber. Therefore,

modes which are supported in the unperturbed fiber abruptly experience increased loss in the region where the pressure is applied. This phenomenon should even be feasible when the pressure is applied isotropically, as in the case of hydrostatic pressure, since the structure of the fibers' holes themselves are not symmetrical. One possible explanation as to why this would occur only when the fiber is subjected to pressure is that the unstressed fiber is in its native state. This is to say that when the fiber was drawn it sought out a geometry which would minimize the stresses within it. As a result, the impact on the mode structure may cause birefringence.

Temperature Insensitivity

The same fiber which was subjected to testing under hydrostatic pressure (DK 02-23) was also tested for temperature dependent loss.[*] A section of fiber was placed through a furnace, with white light propagating through the fiber. The furnace was then heated, with spectra taken on an Ando Optical Spectrum Analyzer. Samples were taken at the initial room temperature, and then at 200 degree C intervals up to 1000. The furnace was then cooled and samples were taken at 200 degree intervals again. The raw data can be seen in Figure 38.

---

[*] Thanks are given to Jeong Kim for his efforts in this phase of the research.

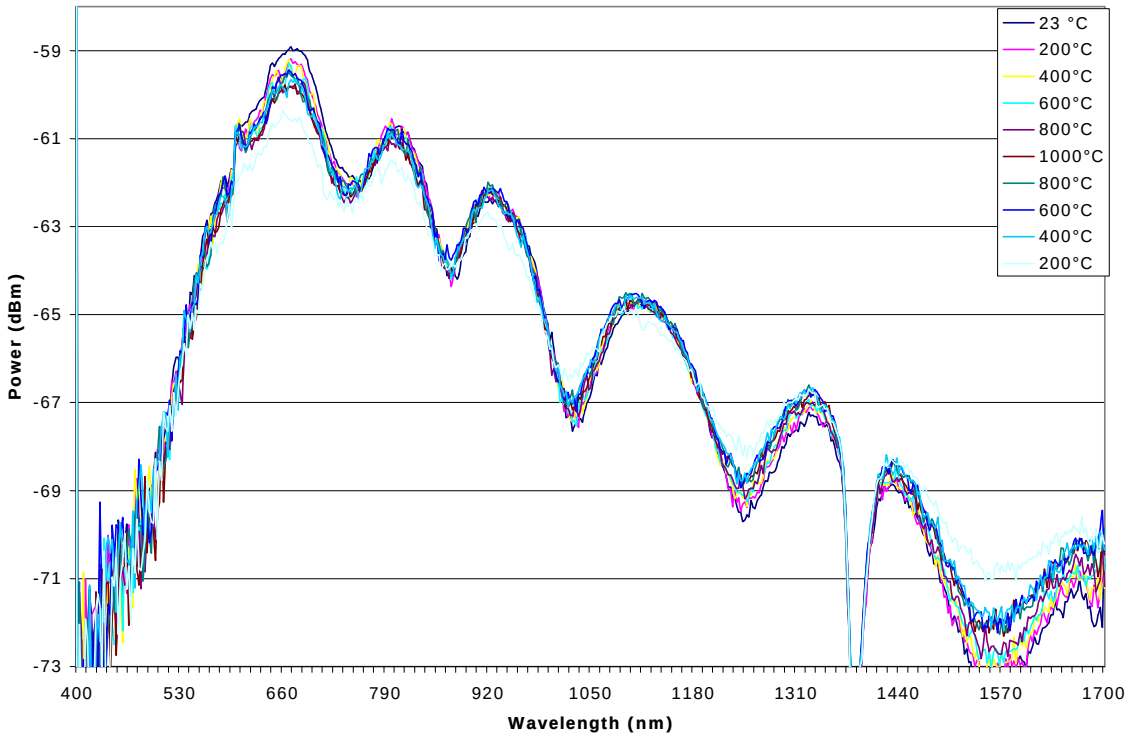

Figure 38: Transmission Spectra of DK 02-23 as a Function of Temperature

In order to determine the presence and amount of temperature dependence which is present in the transmission spectrum, each of the spectra was subtracted from the scan which was taken at 1000°C. These traces can be seen in Figure 39.

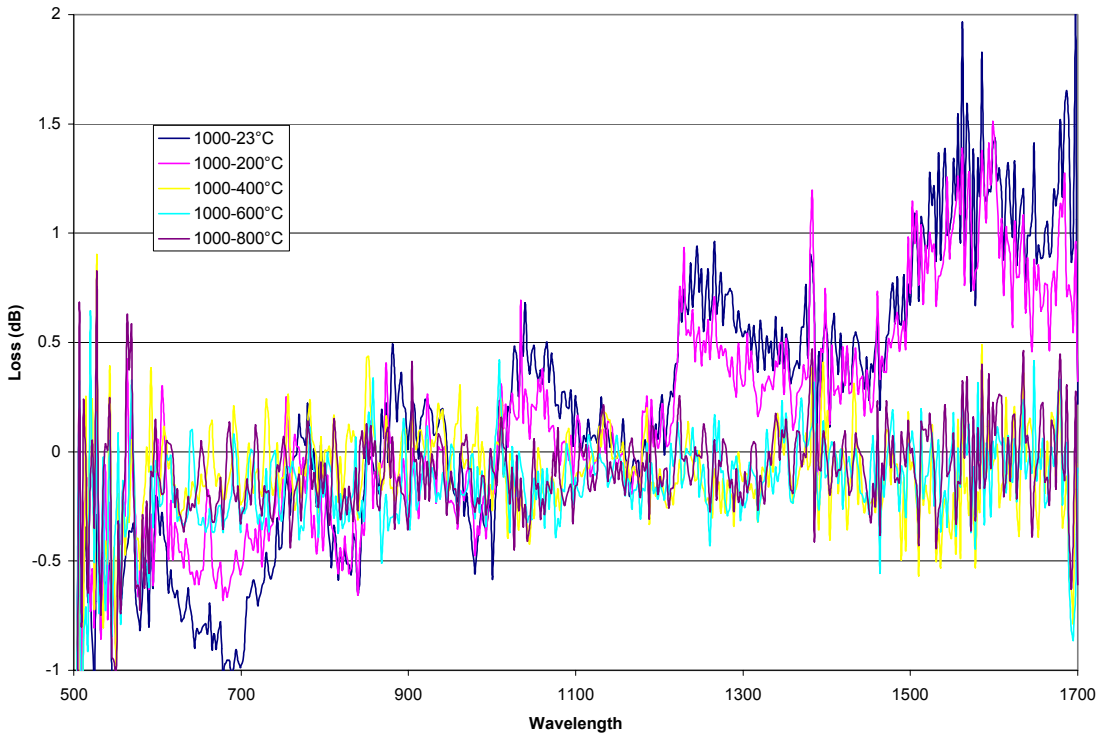

Figure 39:Relative Loss of DK 02-23 as a Function of Temperature (Referenced against 1000°C)

One notes in this figure that there are two groupings of traces. There is a grouping of three traces which are centered on the 0 dB line. This indicates that the temperature dependent loss of the fiber between 400 and 1000°C is below the level of noise in the measurement (the average value for these traces is -0.09428 dB, with an average standard deviation of 0.15620). The other grouping of traces, representing measurements taken when the sample was 23 and 200°C, respectively, are also tightly clustered. This is further demonstrated in Figure 40, where the data has been replotted to show the abrupt transition in loss distribution which occurs between 200 and 400°C. Note that the convergence of all series to a value of 0 at 1000°C is merely an artifact of the fact that I choose that temperature to act as my reference point.

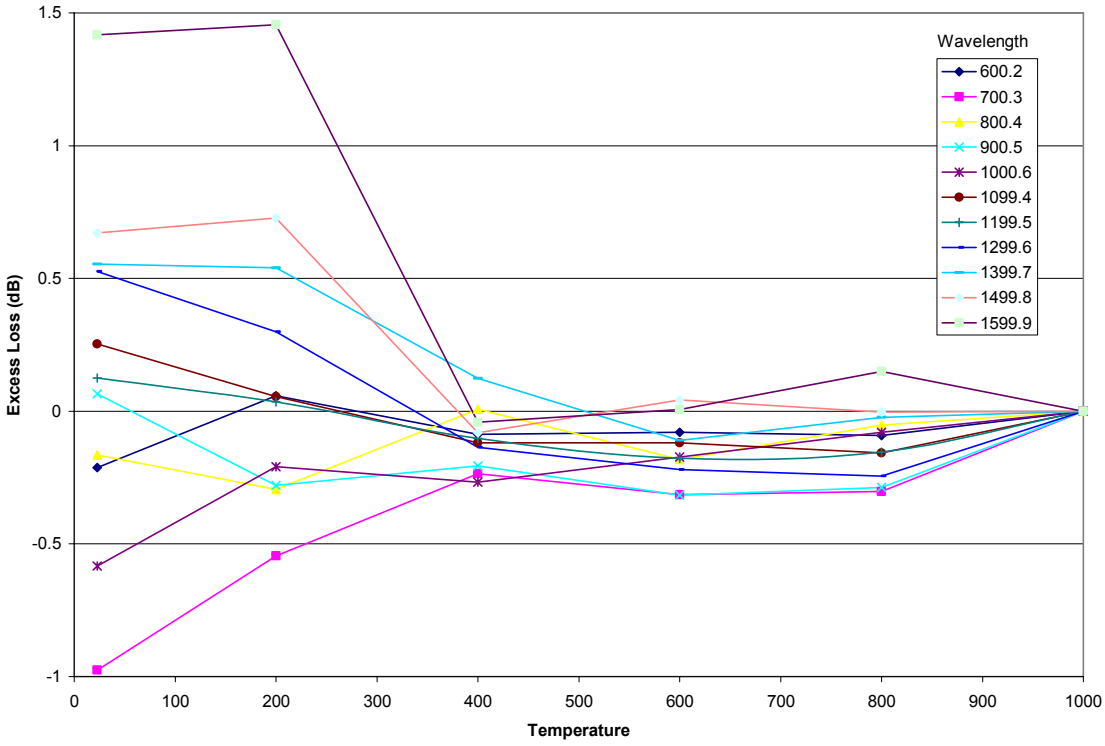

Figure 40: Temperature Dependent Loss Vs. Temperature (as a Function of Wavelength)

Taken together the data indicates that the fiber remained unchanged between room temperature and 200°C, then underwent a measurable change between 200 and 400°C, then remained unchanged up to 1000°C. This was a source of significant confusion, until I later determined that the student who had performed the measurements had not removed the polymeric jacket from the fiber before the test. While not conclusive, it is highly probable that the source of the change between 200 and 400°C was the destruction of the acrylate coating on the fiber.

References:

[1] L.G. Cohen and S. J. Jang, "Interrelationship Between Water Absorption Loss And Dispersion In Multimode Fiber," Applied Optics **20**, 1635-39 (1981).

[2] See, for example: L.G. Cohen and C. Lin, "Pulse Delay Measurements In The Zero Material Dispersion Wavelength Region For Optical Fibers," Applied Optics **16**, 3136-39 (1977).
[3] See, for example: Pollock, C. R. *Fundamentals of Optoelectronics*, Irwin, Chicago, 1995.
[4] Agrawal, G. P. *Fiber-Optic Communications System (Second Edition)*, Wiley-Interscience, New York, 1997.
[5] A. Ferrando, E. Silvestre, P. Andres, J. Miret, and M. Andres, "Designing the Properties of Dispersion Flattened Photonic Crystal Fibers," Optics Express **9**, 687-697 (2001).
[6] J.C. Knight, "Photonic Crystal Fibers," Nature **424**, 847-851 (2003).
[7] N. Mortensen, M. Nielsen, J. Folkenberg, A. Petersen, and H. Simonsen, "Improved Large-Mode-Area Endlessly Single-Mode Photonic Crystal Fibers," Optics Letters **28**, 393-395 (2003).
[8] J. Knight, T. Birks, P. Russell, and D. Atkin, "All-Silica Single-Mode Optical Fiber With Photonic Crystal Cladding," Optics Letters **21**, 1547-49 (1996).
[9] V. Rastogi and K. Chiang, "Holey Optical Fiber With Circularly Distributed Holes Analyzed By The Radial Effective-Index Method," Optics Letters **28**, 2449-51 (2003).
[10] A. Abeeluck, N. Litchinitser, C. Headley, and B. Eggleton, "Analysis of spectral characteristics of photonic bandgap waveguides," Optics Express **10**, 1320-33 (2002).
[11] P. Russell, "Photonic Crystal Fibers," Science **299**, 358-362 (2003).
[12] See any text on mode propagation in optical fibers.
[13] See, for example, Francis To So Yu and Shizhuo Yin, Ed., *Fiber Optic Sensors*, Marcel Dekker Inc, New York (2002).
[14] J. Ma, W. Tang, and W. Zhou, "Optical-Fiber Sensor For Simultaneous Measurement Of Pressure And Temperature: Analysis Of Cross Sensitivity," Applied Optics **35**, 5206-10 (1996).
[15] Frank M Haran, Jason K Rew and Peter D Foote, "A Strain-Isolated Fibre Bragg Grating Sensor for temperature compensation of fibre bragg grating strain sensors," Meas. Sci. Technol. **9,** 1163–1166 (1998).
[16] L. Jeunhomme, M. Fraise, and J. P. Pocholle, "Propagation Model For Long Step-Index Optical Fibers," Applied Optics **15**, 3040-46 (1976).
[17] See, for example: "Encyclopedia of Laser Physics and Technology," http://www.rp-photonics.com/encyclopedia_r.html, or a discussion of the Sellmeier formula.
[18] W. A. Gambling, D. N. Payne, and H. Matsumura, "Mode Conversion Coefficients In Optical Fibers," Applied Optics **14**, 1538-42 (1975).

Crucible Technique

One area of interest in nonlinear optical fibers is the problem of incorporating highly nonlinear materials into the fiber. By utilizing a glass with a high nonlinear refractive index n_2, the strength of the nonlinear effects which occur in the fiber can be enhanced. This increase in the nonlinear optical efficiency results in the same effect being accomplished at a much lower value of the power-length product.

One of the characteristics which is associated with a high nonlinear refractive index is a high linear index.[1] This combination of characteristics poses a difficulty in the fabrication of fibers which use these materials. The single mode core diameter is dependent on the difference in the linear refractive indices between the core and the cladding.[2] The larger this difference is, the smaller the core of the fiber needs to be in order to demonstrate single mode behavior. There are two possible ways of dealing with this index difference. One is to find a suitable cladding material which has a similar, but slightly lower, refractive index. Because the refractive indices are close in value, a fiber can be made with a nominal core diameter (e.g., around nine microns). One of the issues associated with this is the need to find a compatible glass to use for the cladding.[3] These higher index glasses do not have the beneficial structural properties of silica, particularly high strength and ease of splicing, and, as a result, any fiber which is comprised of these materials sacrifices those qualities. [4]

An alternative approach is to generate a fiber which has a high index core surrounded by a lower index material, such as silica. In this case, however, it is necessary to have a very small core to cladding ratio. Normally this is achieved by successively drawing a preform to cane and overcladding it with a tube, to further reduce the ratio.[5] In some instances this cannot be accomplished due to the thermal and mechanical properties of the two materials which are being used. One solution to this difficulty is the crucible technique. By preventing the fusion of the two materials until a time when they are actually being drawn into fiber, the high stress is never applied to the glass, thereby preventing the shattering of the material.

Issues of Fabrication

Despite the beneficial optical properties of high nonlinearity glasses, such as Lead Indium Phosphate (LIP) glass, many possess a number of attributes which make them difficult to manufacture into a fiber. Many of these properties are common to the high nonlinearity, non-silicate glasses, so I will use the example of LIP as a representative case to clarify. Amongst these properties is an extremely high coefficient of thermal expansion (CTE). LIP exhibits a CTE roughly 22 times greater than that which is found in silica. LIP also melts at a far lower temperature than silica. In order to overcome these obstacles it is necessary to employ unusual techniques in the fabrication of these fibers, and

thus we have developed what I refer to as the crucible technique of preform fabrication.[6]

In the crucible technique, the two materials are kept separate until the very final stage of drawing the preform into a fiber. Each is produced in a batch melt. The preform is assembled by first sealing off the bottom end of a silica tube of suitable thickness. (In the first demonstration of this technique, the silica tube had an ID of 1.3 mm and an OD of 20.8 mm.) A piece of LIP is placed into this sealed tube, or crucible. The preform is placed in the furnace and the temperature is slowly brought close to the range at which a silica preform will bait. While the preform is kept just below the temperature which is required for the silica to soften and bait off, the LIP glass (which has a melting temperature of 900° C) becomes molten and pools in the bottom of the crucible. It is necessary for this pooling to occur because during the melting stage air bubbles will become trapped in the molten LIP. A waiting time of forty minutes allows these bubbles to be released from the LIP glass, allowing for a continuous draw of fiber, with an uninterrupted core.

The preform is drawn into a fiber with a small core diameter. There is some variation of the upper limit on core diameter, ranging from approximately 5 microns up to about 8 microns. The upper limit is due to the large difference in the coefficients of thermal expansion which the two glasses possess. The residual stress will be determined by the following relation:[7]

$$\sigma_r = \frac{1}{r^2}\int_0^r \sigma_z(r')r'\,dr$$

Equation 5: Radial Stress of a Fiber

In Equation 5, r is the radius at which the stress is present and the integrand is given by:

$$\sigma_z = \int_{T_{room}}^{T^*} \frac{E(T)}{1-r(T)}\left[\alpha(r,T)-c(T)\right]dT$$

Equation 6: Longitudinal Stress of a Fiber

In Equation 4, E(T) is the elastic modulus, α is the coefficient of thermal expansion, the limits of integration are room temperature and the higher temperature at which stress begins developing within the fiber, and c(T) is defined by: $c(T)=\int_0^R \alpha(r,T)r\,dr$ with R being the overall radius of the structure. For any given material, the elastic modulus and coefficient of thermal expansion are essentially fixed. As a result, the larger the core of the fiber is, the greater the difference $\alpha(r,T)-c(T)$ will become.

The variation in the upper limit is attributed to minor differences in the draw parameters. Since the fiber's stress increases with an increasing volume of LIP, there is an upper limit beyond which the interface will shatter, as well as demonstrating effects of beading, etc.

Initial work attempted to directly incorporate a high index, highly nonlinear glass as the core of an ordered holey fiber made of Pyrex. In this case, an ordered hole structure was assembled out of Pyrex, with just the central core of the preform replaced with a piece of LIP. It was determined, however, that due to the very low melting temperature of the core LIP glass, the LIP core could not be incorporated directly. During the draw, the core material melted and flowed through the interstitial spaces of the preform, destroying any guiding characteristics of the fiber. Instead, the core would require containment to prevent it from spreading though the holey fiber structure

Formation of a Crucible

A crucible is formed by successively overcladding multiple layers of silica tubes, in order to generate a very thick-walled tube with a small diameter central hole. This hole is sealed off at one end, and the core material is added to the crucible. Once the crucible is formed, the core hole can be coated with a layer of modified chemical vapor deposition (MCVD) silica* in order to have a low loss region of cladding surrounding the core, and thereby reduce the overall losses of the fiber.

---

* Glasses which are deposited using MCVD are exceedingly pure, as they are produced by the oxidation of a precursor chemical (such as silicon tetrachloride) which can have impurity levels that are very low. MCVD is the common mechanism through which much of the extremely low-loss telecommunications preforms are fabricated.

Because of the very high linear index of the core material, the evanescent field extends only a very short distance into the cladding. Therefore, even a very thin layer of ultra-pure silica at the interface will keep nearly all of the optical power from experiencing the higher attenuation caused by the batch melt silica of the crucible.

During the draw the preform is lowered into the furnace while the temperature is kept just below the level needed for the crucible to bait off. By doing this for an extended period the core material is given an opportunity to fine, or allow any bubbles which are formed by the melting of the core to escape from the top of the preform. This process requires a core material that has a sufficiently low viscosity at temperatures below the softening point of the crucible. In general, this is easily satisfied by the low melting temperatures of the core material, which yields a fully molten core.

Lead Indium Phosphate Containing Fibers

Lead Indium Phosphate (LIP) glass is a high optical nonlinearity glass which is promising for use in the development of strong nonlinear interactions. The samples used for this work were made at Oak Ridge National Labs. The material was initially designed to act as a radiation hardened glass.[8] It has a refractive index of approximately 1.85, and a coefficient of thermal expansion which is 22 times greater than that of silica. This data can be seen summarized

in Table 4. Based on the refractive index of the LIP glass, the single mode core diameter for a fiber would be approximately 0.7 μm.

Table 4: Summary of Properties of LIP and Silica

	LIP Glass	Silica
n	1.8	1.45
$n_2 \left(m^2/W \right)$	$\left(\sim 50 \text{ x } n_2^{\text{silica}} \right)$	$3*10^{-22}$
CTE $\left(1/°C \right)$	$12.0*10^{-6}$	$5.5*10^{-7}$
Softening Temp (°C)	460	1670

A silica crucible was formed with an inside diameter of 1.6 mm and an outside diameter of approximately 21 mm. This formed the basis of preform DK 01-01. A micrograph of the fiber drawn from this preform is shown in Figure 41.

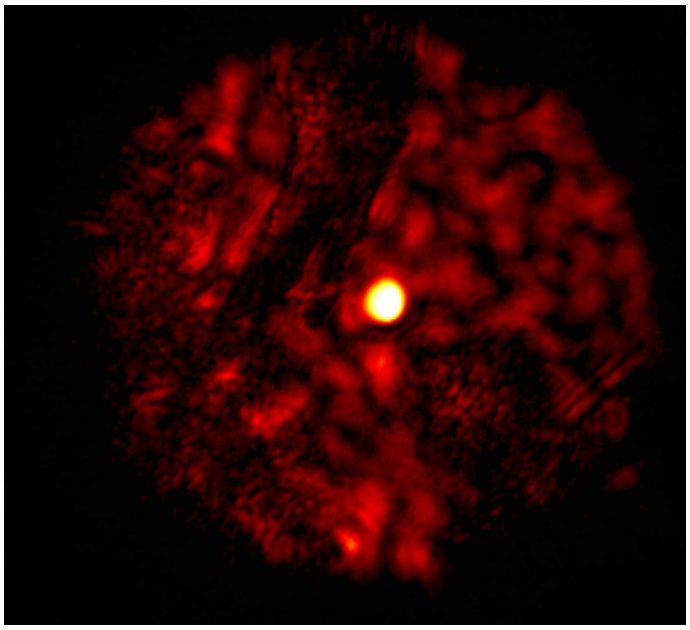

Figure 41: DK01-01

After drawing preform DK 01-01, another layer of overcladding was added to the crucible to make it thicker. This enlarged crucible was then used to form the basis of the preform designated DK 01-06. As with its precursor, the inside diameter is still 1.6 mm but the outside diameter was increased to approximately 24 mm. A micrograph of the fiber drawn from this preform can be seen in Figure 42. Also visible in Figure 42 are some of the assorted layers of overcladding which were used to fabricate the preform. The final preform consisted of seven layers of silica with the LIP core. The rings are visible in the micrograph due to the small variations of the refractive index associated with tube stock from different batch melts.

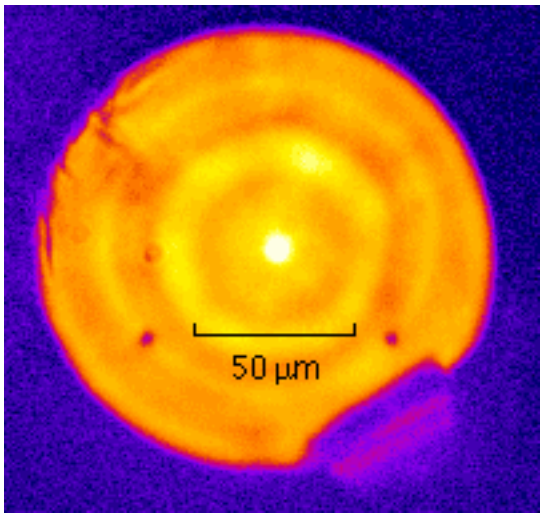

Figure 42: DK01-06

With the LIP core fiber it is necessary for the core to be less than approximately 8 µm, in order to keep the stress low enough to prevent the core from shattering. There is some variation in this value (roughly estimated at 25%), which is most likely due to microscopic variations in the strength of the materials or the rate at

which the fiber cooled during the draw, which could result in annealing some of the stress out of the fiber.

A transmission spectrum of fiber DK 01-01 can be seen in Figure 43. Because of the high attenuation present in the fiber only a relatively short length of fiber could be used. As a result, it was not possible to strip all of the cladding guided light from the fiber; thus the units of the abscissa are somewhat arbitrary. These are the transmission results for a length of fiber which is approximately half a meter in length. As a result, the spectrum shown here is a partial combination of the transmission of the LIP core and the silica cladding. Some relevant features shown here are the increased loss at shorter, visible wavelengths, and the strong loss peak at 1385 nm which is indicative of the presence of hydroxyl groups. It is worth noting that the loss function in the infrared portions of the spectrum is relatively flat, discounting the water loss peak. This is consistent with the characteristic of the LIP being highly transmissive out to a wavelength of 2.8 μm.

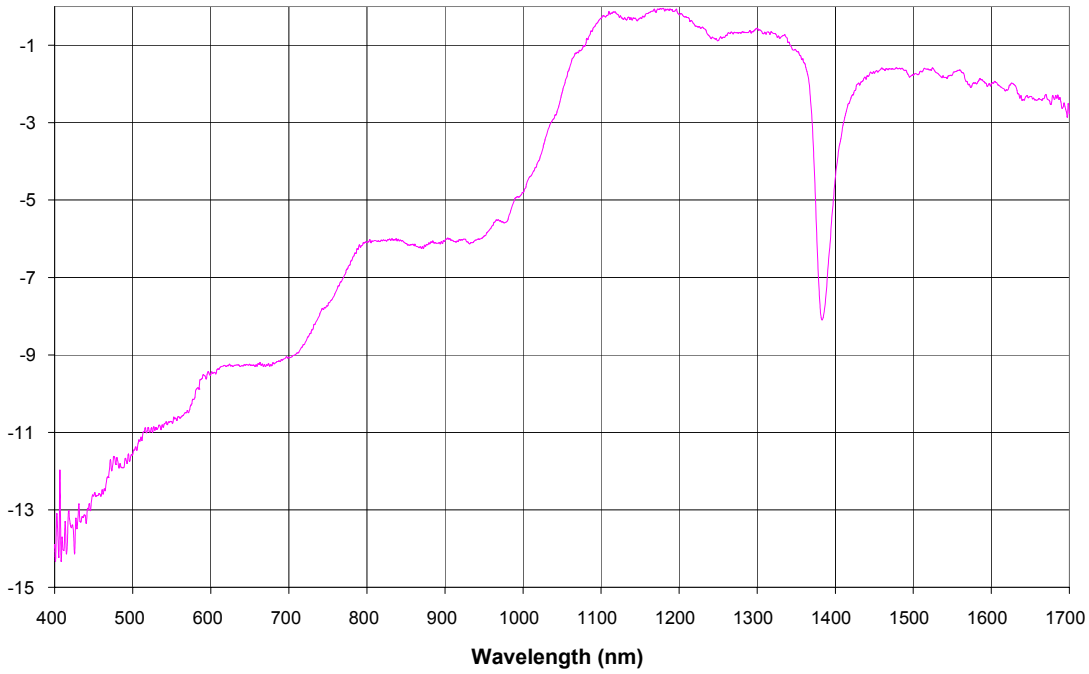

Figure 43: Loss Spectrum of LIP Fiber DK 01-01

MM2 Glass Fiber

Another core material which was used for the crucible technique is Kigre, Inc MM2 glass. This is an erbium doped gain material with a phosphate host.[9] The crucible was formed of silica with an inside diameter of 1 mm and an outside diameter of 11.8 mm.

One unusual aspect of this particular crucible draw is that the remaining preform (which still contained some of the core material) cooled down very slowly over a period of several hours. As a result, the core material did not shatter completely, as some of the stress was annealed out of it. The resulting preform can be seen

in Figure 44. This image was taken on a polariscope to demonstrate the stress birefringence of the preform.[10] The bright areas are regions of high stress, which are separated by regions of low stress due to some bubbles which are present in the core. One can see that this stress extends well outward into the silica cladding region.

Figure 44: DK02-01 MM2 Crucible Preform

A micrograph of the fiber made with MM2 glass can be seen in Figure 45. The core is excited in a LP_{11} mode. Information regarding the gain/loss spectrum of fiber DK 02-01 is not available.

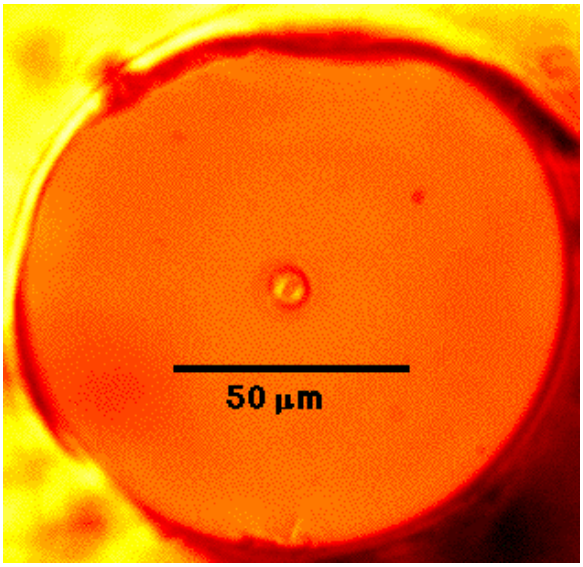

Figure 45: DK 02-01 Micrograph

Tellurium Oxide Glass Fiber

The crucible technique can also be applied in systems where the host glass is not silica. Preforms have been made where the host glass is Pyrex, with a TeO_2 core, although they could not be successfully drawn into fiber. Initial attempts were made to make a fiber with a TeO_2 core in a silica host; however, this was determined to be impossible as the boiling temperature of the tellurium oxide was reached before the softening temperature of the silica.[11] As a result, when the preform was drawn, the powder vaporized and pressurized the preform -- resulting in a blow out of the preform

Following that attempt, some preforms were made of tellurium oxide in a Pyrex host. Initial attempts allowed too much air to be trapped with the powder,

resulting in an unpredictable presence of the core. In order to resolve that issue, the tellurium oxide was pre-melted in the crucible to provide a solid core. Once the core was formed, the preform was drawn as normal, with equivalent results. Attempts with this method using a 5 mm by 9 mm tube were not successful either, due to insufficient strength in the fiber.

Other Glasses

Preforms have been fabricated with a core of Schott F2 glass. Preforms were fabricated in Pyrex and silica hosts. In preform DK 03-06, F2 in a silica crucible, the drawn fiber only exhibited a thin skim of F2 glass surrounding a large central hole. The fiber could not be used for optical guidance due to this. The Pyrex™ preform with F2 was severely deformed, but could be tapered by hand to form a short length of high diameter cane.

Two preforms were also attempted which used a Pyrex™ core, surrounded by a silica cladding. In the first of these two (DK 04-01), the crucible had a 13 mm inside diameter and a 19 mm outside diameter. In this instance the fiber could not be drawn since the silica lacked sufficient strength to support the molten Pyrex™. The second Pyrex-in-silica preform was DK 04-02, which had inside and outside diameters of 4.86 and 8.3 mm, respectively. Although the draw was unstable with regard to the fiber diameter, some lengths of fiber were obtained.

A plot of the loss spectrum of this fiber can be seen in Figure 46.* The features of note in this plot are the high loss peak due to the hydroxyl group (at 1385 nm) and the steadily increasing loss of the fiber as the wavelength becomes shorter. This is likely due to a combination of the inherent loss of Pyrex™ and the tendency for shorter wavelengths to be more heavily scattered by irregularities in the core-clad boundary (Mie Scattering).[12]

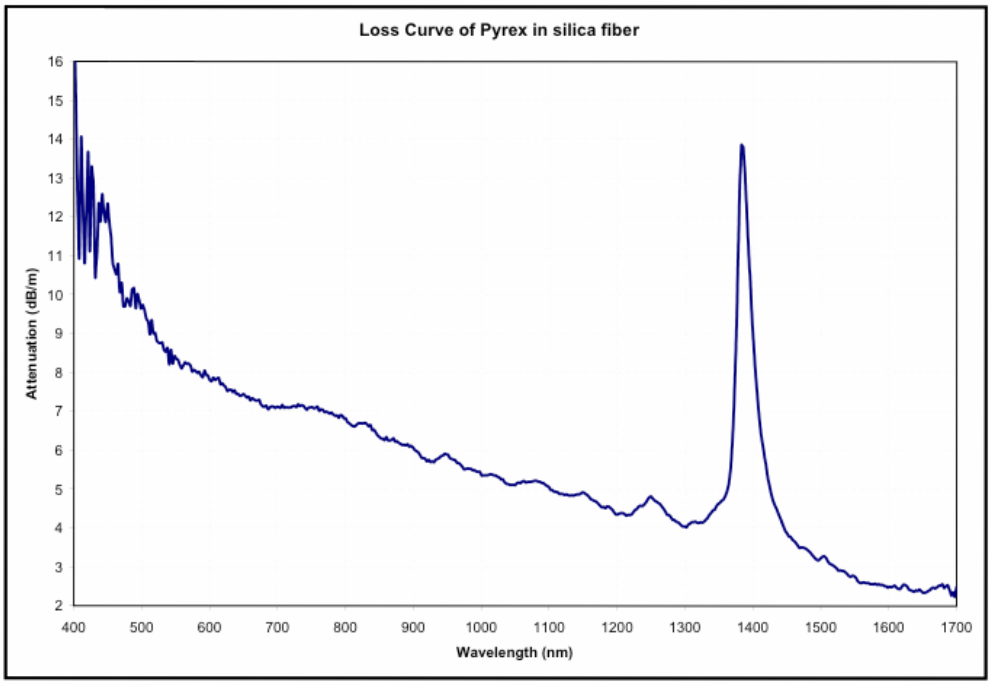

Figure 46: Loss Spectrum of Pyrex-in-Silica Fiber, DK 04-02

Alternate Approach Crucible Technique

A second approach to the crucible technique was developed much later. In this instance the core and cladding materials are allowed to fuse prior to fiber draw.

---

* Thanks to Nitin Goel for the loss measurements of Pyrex™ in silica fiber

The core material is melted in a vessel and the cladding tube is lowered into the melt. A vacuum is then applied to the top of the cladding tube drawing molten core material up into the preform. After the preform has cooled, the bottom is sealed and it can be overclad to attain a thicker overall diameter.

This method was tried on preforms composed of several materials. Some of the materials were highly unsuccessful, whereas others showed more promise. The first preforms of this type which were attempted were Schott SFL6 glass in both Simax™ (a borosilicate glass similar to Pyrex™) and silica tubes. The SFL6 in Simax was never successful, since the temperature needed to melt the core was higher than the working temperature of the cladding tube. As a result, the tube bent and warped during the process of drawing up the SFL6. The SFL6 in silica was successfully drawn up producing preform DK 04-05 (which was never drawn into fiber, due to time constraints).

The second core material that was attempted with this method was a sample of the glass from Fisk University labeled “Sample 3.” The composition of Sample 3 is shown in Table 5. The tube in which this material was drawn up was Simax capillary.

Table 5: Composition of Glass From Fisk University Labeled "Sample 3"

Material	Percent of Composition
PbO	27%
GeO_2	43%

$CaCO_3$	10%
TeO_3	20%

Two preforms of this type were attempted (DK 04-06 and DK 04-07). The primary problem which occurred in these preforms was that the temperature necessary to melt the core glass is approximately the same as the temperature at which the Simax tube becomes soft and begins to bend. As a result, the core material could not be fully molten at the time that it was attempted to be drawn up into the preform. Because the material was so viscous, a significant amount of air was also drawn up the tube with the core material. When the preforms were drawn into fiber, the core consisted only of a thin skim of the Telluride glass on the inside surface of the tube, with a large hole in the center.

A subsequent attempt was made with the alternate crucible technique in a try to draw germania (GeO_2) up into a silica capillary tube. Again the core material could not be gotten to a high enough temperature to melt and be drawn up the preform. In this instance it was due to the upper limit of the temperature range of the muffle furnace which was available at the time, since germania does not melt until a temperature of 1076 °C.[11] In the attempt to make the germania sufficiently molten to be drawn up the tube, the furnace overheated, which resulted in burning out the heating element. At this stage it was decided that the proven feasibility of the original crucible technique was sufficient. While it seems likely

that the suction crucible technique can be further developed successfully, I chose to end my efforts in that direction for the purposes of this research.

References:

[1] Boyd, R. W. *Nonlinear Optics*, Academic Press, Boston, 1992.
[2] Pollock, C. R. *Fundamentals of Optoelectronics,* Irwin, Chicago, 1995.
[3] B.C. Sales, L.A. Boatner, and S.W. Allison, "Lead-Indium Phosphate Glasses for Optical Applications," Proc. SPIE **2287**, Properties and Characteristics of Optical Glass III, Alexander J. Marker; Ed 126-132 (1994).
[4] B. C. Sales and L. A. Boatner, "Optical, Structural, and Chemical Characteristics of Lead-Indium Phosphate and Lead-Scandium Phosphate Glasses," Journal of the American Ceramic Society **70,** 615-621 (1987).
[5] See, for example, "Drawing Optical Fibers," http://www.hikeytech.com/newsletters/fall-02/nl357.pdf
[6] A somewhat related technology, described as the powder in tube method can be found in: John Ballato and Elias Snitzer, "Fabrication of fibers with high rare-earth concentrations for Faraday isolator applications," Applied Optics, **34**, 6848-54 (1995).
[7] P. K. Bachmann, W. Hermann, H. Wehr, and D. U. Wiechert, "Stress In Optical Waveguides. 1: Preforms," Applied Optics **25**, 1093-98 (1986).
[8] B.C. Sales and L.A. Boatner, "Lead Phosphate Glass as a Stable Medium for the Immobilization and Disposal of High-Level Nuclear Waste," Materials Letters **2**, 301-304 (1984).
[9] Data on Kigre MM2 available at http://www.kigre.com/MM2Datasheet.pdf
[10] M. Saunders, "Determination of the stress in optical fibers by means of a polariscope," Review of Scientific Instruments **47**, 496-500 (1976).
[11] Lide, D.R., *CRC Handbook of Chemistry and Physics*, *73rd Edition*, CRC Press, Boca Raton, 1992.
[12] Agrawal, G. P. *Fiber-Optic Communications System (Second Edition)*, Wiley-Interscience, New York, 1997.

Applications of Random Hole Optical Fibers and Crucible Technique Fibers

The random hole optical fiber (RHOF) and the crucible technique fiber (CTF) each have independent applications. The RHOF, due to its innate pressure sensitivity, shows great potential in the area of fiber sensors. The CTF also has great potential in nonlinear optical systems, such as all-optical switching. Likewise, the two technologies could be used in conjunction to generate additional devices such as the double clad amplifier fibers.

Sensor Suite Based on Random Hole Optical Fibers

Based on the inherent pressure sensitivity of the RHOF, a whole collection of sensors can be developed. There are two characteristics which are necessary to have a suitable fiber-based sensor. The first attribute is a mechanism to provide a calibrated measurement.[1] If a system does not have any inherent calibration, then when a loss in power is detected it is impossible to determine the cause. The reduced power output could be caused by the fiber being subjected to pressure, another source of fiber loss, or by the degradation of the aging light source used to illuminate the fiber. Because the pressure sensitivity in RHOF is wavelength dependent (having greater pressure induced loss at shorter wavelengths), the fiber can be used in a calibrated manner. In an example device, light can be launched at two wavelengths, one which is more sensitive to pressure (such as 600 nm) and another which is far less so (such as 1550 or 1700 nm), thus providing for calibration.

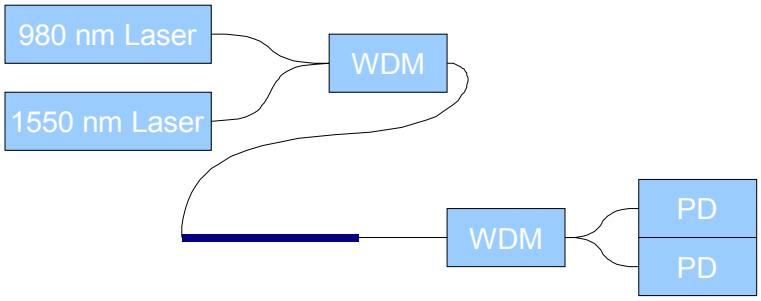

Figure 47: Notional Pressure Sensor Based on RHOF

While fiber sensors have been around for decades, there has always been a primary limitation to them. In general, the sensitivity to pressure is matched with a corresponding temperature sensitivity.[1] This is well demonstrated in a Bragg grating in a fiber. The Bragg grating is a narrow wavelength reflector which is encoded into the fiber. The reflected wavelength is determined by the period or spacing of neighboring index variations. As a result, when the fiber containing the grating is stretched, the period of the fringes increases, and thus the wavelength which is reflected becomes longer. The response to strain is given by: [1]

$$\frac{\Delta\lambda_B}{\lambda_B} = P_e\varepsilon + \left[P_e\left(\alpha_s - \alpha_f\right) + \varsigma\right]\Delta T$$

Equation 7: Response of a Fiber Bragg Grating to Strain and Temperature (Here, λ_B is the Bragg wavelength, P_e is the strain-optic coefficient, α_s and α_f are the coefficients of thermal expansion of the substrate that the fiber is bound to, and the fiber itself, respectively, ς is the thermo-optic coefficient, and T is the temperature.)

As one can see in the first portion of Equation 7, the Bragg wavelength increases with increasing strain. This corresponds to the strain physically elongating the fiber, moving the maxima of the refractive index variations further apart.

However, when the temperature of the fiber increases, the fiber also expands as determined by the coefficient of thermal expansion. Then the period of the Bragg grating is again increased, which also results in a shift of the reflected light to longer wavelengths. Therefore, when the sensor returns a reading of increased reflected wavelength, it is impossible to know whether it is due to the stretching of the fiber or a rise in the fiber's temperature. As a result, it has always been necessary to have two sensors in order to be able to compensate for the impact of the undesired variable.

Because the RHOF possesses pressure sensitivity without the corresponding temperature response, it is imminently suitable for use in sensor systems. Depending on the housing constructed for the sensor, such a fiber can be used to measure any of a number of variables. Examples: By simply placing a weight distributing object on the fiber, the fiber can sense pressure or weight. For higher pressures, the fiber can be used directly without any special housing at all since it responds to hydrostatic pressure as well. To measure temperature, the fiber is placed within a material with a known coefficient of thermal expansion. When the material heats and expands it will apply pressure to the fiber.

All Optical Switch Based on Crucible Technique Fiber

Another application for the specialty fibers is the category of nonlinear switches and filters -- which can separate a group of pulses from the train of data in a fiber. This is often used, for example, in time division multiplexing, where a single fiber will be carrying many data streams simultaneously and at the same wavelength.[2] In a simplified system, one can consider a case where the fiber is carrying data from ten separate signals. A fixed time duration of the data stream is allocated to each set of sub-data. Then this data reaches a switching location where only one set of data is needed. One solution is to detect all of the data, extract that which is needed, and then retransmit all of the other data to its destination. However, this is a complex process which requires computation, as well as the expenditure of money required to install a full, electronic repeater (i.e., signal conditioners, a transmission system, etc.)

It is desirable to establish an all optical switching system, which allows a single set of the data to be detected, and all others to continue on the original fiber. One type of approach to this utilizes the nonlinear refractive index of fibers. One such method for achieving this is using what would be considered an LP_{01}-LP_{02} mode filter.[3,4] A schematic of the general layout of such a switching system can be seen in Figure 48. The incoming data is first amplified so that the data which is left on the transmission system won't be excessively diminished by tapping off a portion of the power. After this portion of the signal is tapped off by a fiber

coupler, the remainder, which is the ongoing data, continues on. The portion which is extracted is what will be used to detect the needed data.

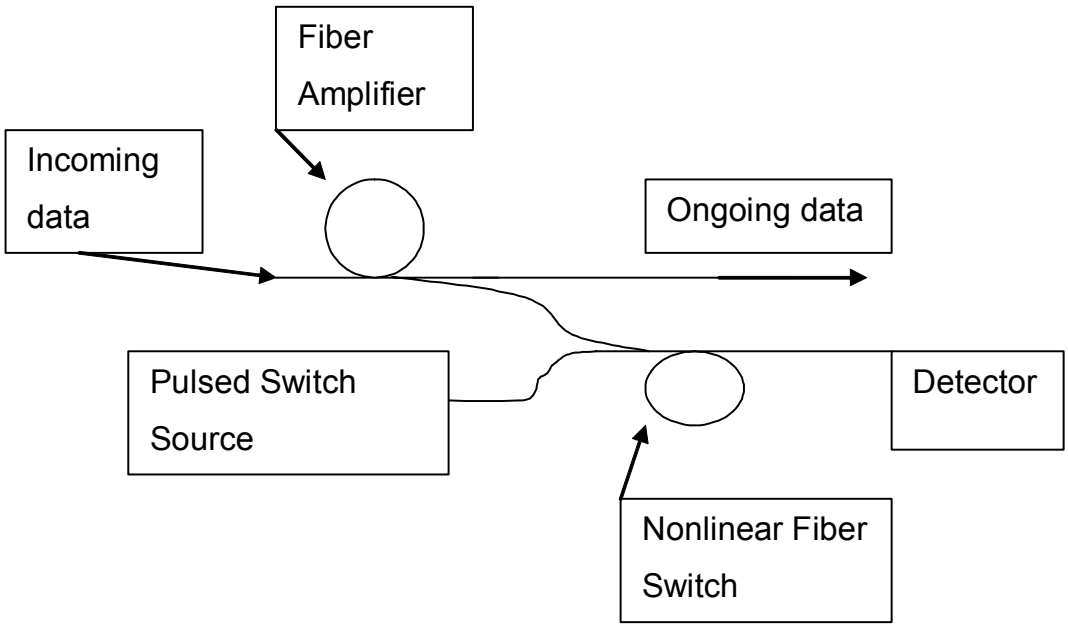

Figure 48: Schematic of Operational Use of Nonlinear Switch

The functioning of an LP_{01}-LP_{02} is based on the host fiber supporting just two modes. The first two circularly symmetric modes which will occur in a fiber are LP_{01} and LP_{02}. A representation of their respective field distributions can be seen in Figure 49. The profile of LP_{01} is nearly Gaussian, while that of LP_{02} is a similar Gaussian with a ring surrounding it, although properly they are Bessel functions.[5] Because the two modes have different propagation constants, they will interfere with each other as they travel along the fiber. When the modes are "in phase" the fields in the center will interfere constructively, resulting in a strong, on the axis spot. When they are "out of phase" the center of the distributions will cancel each other, leaving only the ring portion of the LP_{02} mode distribution.[2] As a

result, when an aperture is placed at the output of the fiber, the amount of power which makes it through the aperture is determined by the relative phases of the two modes at that point. The simplest mechanism of providing the aperture at the end of the fiber is to splice the switch to a piece of single mode fiber. The single mode fiber can only be coupled to by fields which are propagating in a fashion which is close to single mode fiber's mode field (which is the LP_{01} mode).

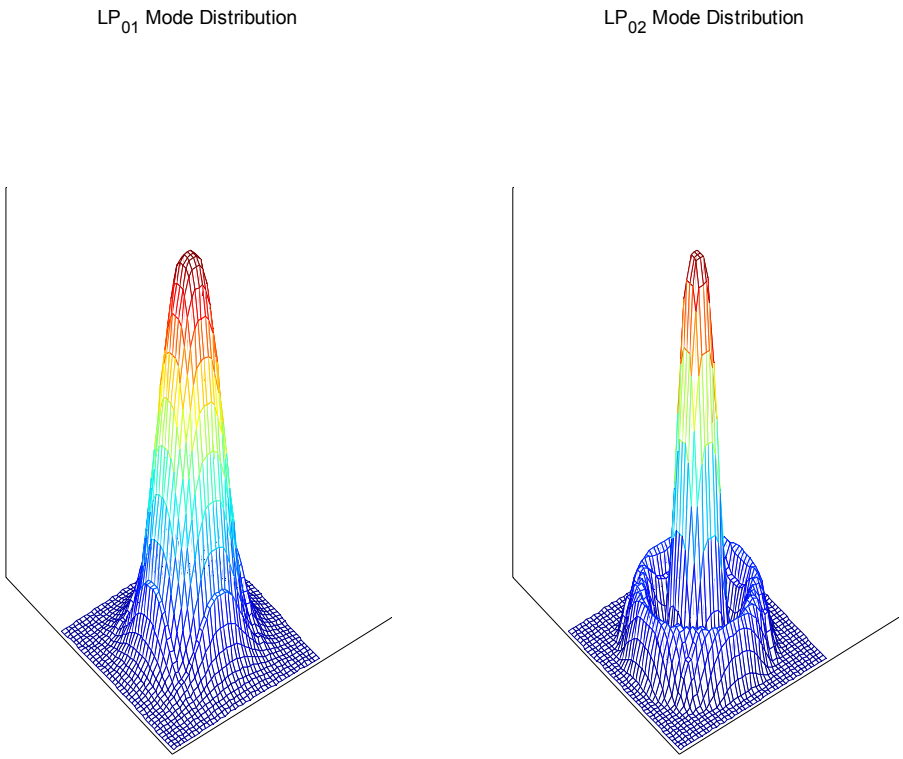

Figure 49: Profiles of Modes LP_{01} and LP_{02}

In the case of a nonlinear switch, an added component to this process is created by altering the refractive index of the fiber in which the modes are beating. The total refractive index in the case of a nonlinear material can be expressed as:

$$n = n_0 + n_2 I$$

Equation 8: Nonlinear Refractive Index

where n is the total refractive index, n_0 is the linear component, n_2 is the nonlinear refractive index, and I is the intensity of the light which is present. Because the propagation constant of the fiber is determined by the refractive index, shifting the refractive index will, in turn, change the beat length of the two modes. In general, as the power becomes higher, the beat length of the fiber will become shorter. A schematic of this can be seen in Figure 50. The aperture depicted in Figure 50 can be easily realized by simply splicing the dual mode fiber to a single mode fiber having the appropriate core diameter.

In order to operate the switch, the pulsed switch source in Figure 48 is timed to be active at the same time that the desired data is going to enter the switch. The high intensity from the switched source will act to alter the refractive index, as described in Equation 8. As the refractive index changes in the fiber, the propagation constant for each of the two modes changes. In general, as the intensity of the switching pump increases, the total refractive index will also increase. As this happens, the effective index for the higher order mode (LP_{02})

will increase more rapidly than that of the lower index mode (LP_{01}). This is what results in the shortening of the beat length.

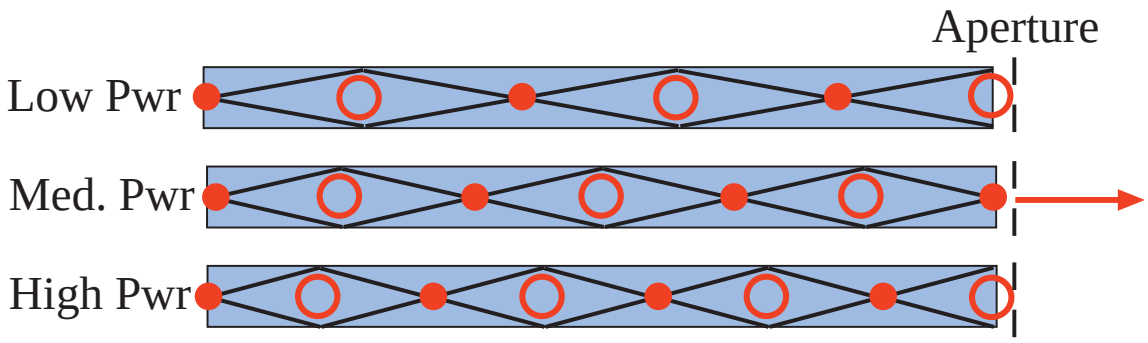

Figure 50: Beating of Modes in a Dual Mode Switch/Filter

This system can be used in a number of fashions. One is in the externally modulated manner described above and shown in Figure 48. Another application is to filter some of the variations from a signal.[6] As a signal travels along a fiber, it experiences both loss and the accumulation of noise. While amplifying the signal to compensate for the loss with a device such as an Erbium doped fiber amplifier (EDFA), it also amplifies the noise, as well as adds additional noise. As the noise becomes more significant, the ability to detect whether the received signal is a zero or a one is degraded. Once this degrades to a certain degree, the data contained within the signal is not retrievable.

In order to enhance the ability to extract data from the signal, it is desirable to remove some of the noise from the data stream. In this case the switch fiber will operate in a fashion more precisely akin to that depicted in Figure 50. Only when the power entering the fiber in the “medium power” range does the light

successfully make it through the system. The use of the fiber in this fashion will have two benefits. First, by reducing the high power spikes which occur in the case of noise on top of a "one" signal, it lowers the likelihood of saturating the detector, and increases the response time.[7] Second. the other function that it will serve is to clean the "zero" data values, and impose a floor on the signals which are below the necessary threshold. By incorporating these optical switches periodically into the system, one can prevent the accumulation of noise spikes during the "zero" values, removing the possibility of detecting a false "one".

All of the items discussed above are feasible in a standard germanosilicate fiber. However, using a crucible technique fiber permits one to use much shorter lengths to accomplish a comparable effect. For a particular application, the product of the fiber length with the nonlinear efficiency is a constant.[8] There are two reasons why a 'crucible technique' fiber can be much shorter than a standard telecommunications fiber and still obtain the same effect. These two considerations are illustrated in Equation 9.

$$NLO_{eff} \sim \frac{Pn_2}{A_{eff}}$$

Equation 9: Dependency of Nonlinear Optical Efficiency

In this equation NLO_{eff} is the efficiency of the nonlinear interaction, P is the optical power which is driving the nonlinearity, n_2 is the nonlinear refractive index of the core material, and A_{eff} is the effective area of the fiber. The effective area,

for a given wavelength and mode, is approximately proportional to the area of the fiber's core. The first reason why a 'crucible technique' fiber can be much shorter than a standard telecommunications fiber (which is commonly used due to its prevalence) is that the nonlinear index n_2 of a crucible technique core is much higher than that which is found in standard silicate, or germanosilicate, glasses. Secondly, because the linear index of the crucible technique materials is so much higher (sometimes with differences in refractive index, Δn, greater than 0.4), the core diameter of fibers made from these materials must be much smaller to obtain the same modal structure. Therefore A_{eff} is much smaller, also increasing the nonlinear efficiency. The beat length of the fiber is inversely proportional to the nonlinear optical efficiency.

Although the value for n_2 is not known for most of the materials that have been tested with the crucible technique, the similarities of these materials to known lead and phosphate glasses lead us to believe that they possess roughly fifty times the nonlinearity of silica.[9] Combining this with the smaller core diameter, one can achieve total improvements in the nonlinear efficiency of up to a factor of a thousand. As a result, for a given optical power (such as 1 Watt), the same nonlinear effect can be achieved in 0.1% of the length of fiber -- 1 meter rather than a kilometer.

Random Hole Fibers and Crucible Technique Fibers for Double Clad Fiber Amplifiers

A third category of application for the specialized fiber is where the two processes are combined. This is the primary area in which the originally intended combination of the two technologies researched in this program can be successfully combined to serve a function. A schematic of such a fiber can be seen in Figure 51. The structures which are present, progressing from the center outwards, are the core (which is made of crucible technique material), the inner clad (which is the silica crucible), the pore band (which is fabricated by generating a random hole fiber layer), and the outer confinement tube (again, silica to hold the powder). The green lines in the inner clad represent the pump light which is injected into the fiber to power the amplification.

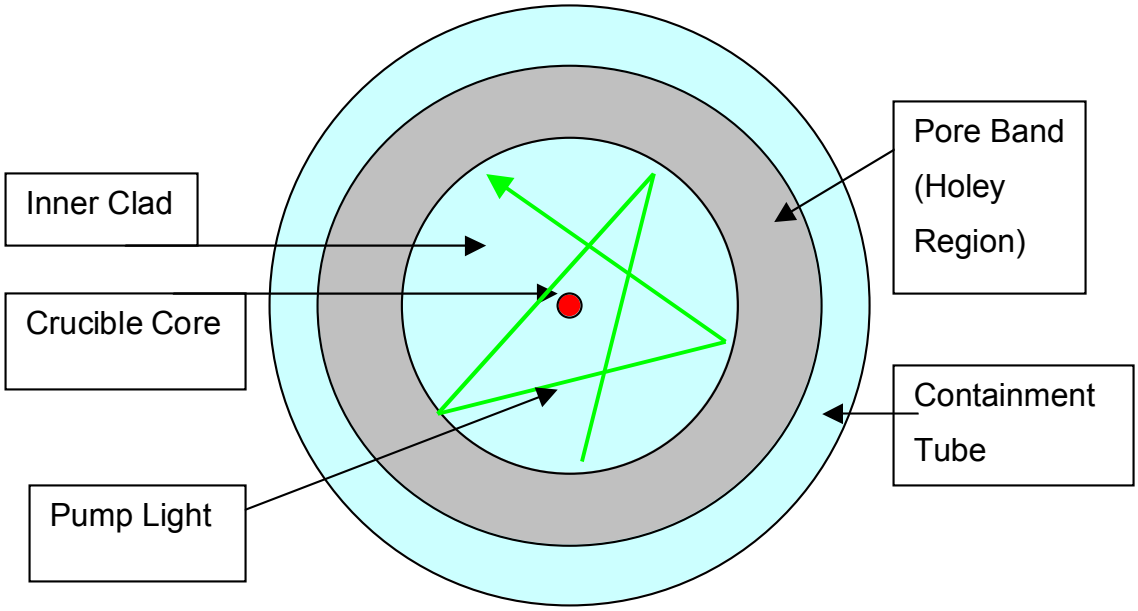

Figure 51: Schematic of Double Clad Amplifier Fiber Using Holey Structure and Crucible Technique Core

Fabricating such a preform begins by generating the crucible which will form the inner cladding. Once that is constructed, it can be concentrically fused inside a larger, relatively thin walled tube. The powder with gas producing material is then poured into the space between the two layers, to ultimately form the outer cladding. Finally, the piece of core material is inserted into the central hole of the crucible. Once the preform has been assembled in this fashion, it can be placed on the draw tower and drawn to fiber. During the draw process the core is melted and any trapped gas escapes, while the gas producing agent oxidizes and generates the porous cladding.

There are independent reasons why each of these two technologies are so suitable for use in double clad amplifier fibers. First, using the holey region, or pore band, for the outer cladding results in allowing the pump light to be injected with a very high numerical aperture (NA). The benefit of this is that the higher the NA of the fiber, the more easily light can be coupled into the fiber and consequently the larger the source that can be used to pump the amplifier. The use of a larger source allows for greater optical powers to be coupled into the fiber and thus for greater potential amplification. Additionally, the high NA means that light confined by the outer cladding can propagate across that region at a steeper angle, resulting in more pump light absorption in the core, per unit length.

The major benefit of using the crucible technique to produce the core of the double clad fiber is the freedom it allows in choice of core materials. I will

address the example of an Erbium doped fiber amplifier (EDFA). In a typical EDFA (meaning one in a silicate host) there is a strict limit on the amount of Erbium which can be incorporated successfully into the glass.[10] One limiting factor is the point at which phase separation of the glass occurs.[9] At concentrations which are much lower than that necessary for phase separation, concentration quenching occurs. Concentration quenching happens because the Erbium in a silicate host tends to form clusters within the glass. When the clusters become too large, the excitement of the Erbium ions gives way to various non-radiative mechanisms of relaxation. Amongst these are parametric upconversion, and OH-quenching. The benefit of the crucible technique materials is that they do not suffer the concentration quenching issue that the silicate glasses do. Phosphate glasses, in particular, can have very high concentrations of Erbium, which allows for extraordinarily large degrees of gain. One such material is the Kigre MM2™ glass with which preform DK 02-01 was fabricated.

Such a fiber has great potential for application in amplifier systems. Likewise, any system which demonstrates optical gain has the potential to form the basis of a laser. In order to convert a fiber amplifier into a fiber laser, all that is required is to add some mechanism of optical feedback to the system. Thus, any mechanism which retroreflects a substantial portion of the optical power within the fiber can be used. A common means of doing this is through splicing fibers with Bragg gratings onto each end of the fiber amplifier. The benefit of such a

system is that it exists as a single structure, making it impervious to misalignment by vibration or any impact which does not fracture the glass.

References:

[1] See, for example, Francis to So Yu and Shizhuo Yin, Ed., *Fiber Optic Sensors*, Marcel Dekker, New York, 2002.
[2] Agrawal, G. P. *Fiber-Optic Communications System (Second Edition)*, Wiley-Interscience, New York, 1997.
[3] H.G. Park, C.C. Pohalski, and B.Y. Kim, "Optical Kerr switch using elliptical-core two-mode fiber," Optics Letters **13,** 776-778 (1988).
[4] Also derived from conversation with Dr. Roger Stolen.
[5] See, for example, Richard C. Dorf, Ed., *The Handbook of Optical Communications Networks*, CRC Press, Boca Raton (2003).
[6] P. Petropoulos, T. M. Monro, W. Belardi, K. Furusawa, J. H. Lee, and D. J. Richardson, "2R-regenerative all-optical switch based on a highly nonlinear holey fiber," Optics Letters **26,** 1233-35 (2001).
[7] Pollock, C. R. *Fundamentals of Optoelectronics*, Irwin, Chicago, 1995.
[8] Boyd, R. W. *Nonlinear Optics*, Academic Press, Boston, 1992.
[9] See, for example, Marvin J. Weber, Ed. *Handbook Of Optical Materials,* CRC Press, Boca Raton, 2003.
[10] See, for example, Marvin J. Weber, Ed. Handbook Of Lasers, CRC Press, Boca Raton, 2001.

Conclusions and Recommendations for Future Work

The primary conclusion to be drawn from the work completed for this dissertation is that new methods have been developed in this work for producing optical fibers with original characteristics. At the same time, both the techniques for fabricating random hole optical fibers (RHOF) and those for fabricating crucible technique fibers, are rife with potential pitfalls.

Conclusions Relating to the Fabrication of Random Hole Optical Fibers

The course of this research has demonstrated that there exists a grouping of methods of failure which are particularly inimical to the successful fabrication of Random Hole Optical Fibers (RHOF). These mechanisms can be loosely grouped in the following issues:

- Insufficient cladding density to maintain the localization of the core

  This was demonstrated by the attempts to fabricate fibers where the cladding was comprised of aerogel material. Uniformly in attempts which used aerogel for the cladding, the core migrated through the cladding region to fuse with the outer wall, even when attempts were made to localize it with high density silica disks. This method of failure was also observed in the attempts to fabricate fibers whose cladding was comprised entirely of microbubbles.

- Excessive moisture retained in powdered material

This conclusion is drawn from the failures of the sol-gel powder derived preforms. In the case of both preforms which were attempted of this material, moisture condensation was readily visible inside the preform tube where it left the furnace. In both cases the preform suffered blowouts of the side wall. At the same time, when droplets of condensed water fell down the inside of the preform, they could be heard to strike the heated region of the preform with a sound similar to a miniature explosion.

- Contamination of material that raises the cladding refractive index

  Evidence of this was seen in one preform successfully drawn whose cladding was fabricated of mixed silica and microbubbles. The presence of the aluminum from the microbubbles caused the cladding region to have an overall higher refractive index than the core, effectively preventing guidance in the core of the fiber.

- Excessive gas present during cladding formation

  This was demonstrated by a vast number of preforms. This mechanism of failure, which resulted in either blowouts or an unsuitable fiber cladding, was seen in preforms which contained 325- mesh silica as well as preforms which contained an excess amount of fining powder (gas producing agent). One attempted remedy of this situation was to apply vacuum to the preform before drawing it in an attempt to eliminate excess gas, but this was found to be of very marginal benefit.

- Insufficient gas present during cladding formation

  This conclusion is drawn from the results of preforms which used coarse silica powder without fining material, as well as those which used an insufficient amount of fining agent. In these cases there were not a sufficient number or density of holes formed to act as an effective cladding.

Despite the existence of these mechanisms which lead to failure in the fabrication of RHOF, it has also been amply demonstrated that it is fully possible to successfully fabricate the RHOF, in a controlled and repeatable fashion. Through a suitable choice of host powder, a carefully determined set of proportions of fining agent to silica, and attention to the draw parameters of furnace temperature and draw speed, the competing forces which develop during fiber draw can be balanced to result in a fiber which is acceptably durable, and guides light. Furthermore, repeating the steps of fabrication consistently results in the production of fiber with similar characteristics (although due to the random nature of fabrication, the geometry is necessarily different between samples).

Recommendations for Further Research in the Area of Random Hole Optical Fiber Fabrication

One area in which further research could distinctly be of benefit in the continuing evolution of RHOF is finding new methods for attaining a more uniform distribution of gas producing agent. One such line of research, which is currently

being undertaken with the supervision of Dr. Gary Pickrell, is based in the use of polymeric precursors for the cladding material. This work is being accomplished by suspending the silica in a liquid matrix. The composition of this matrix is such that when it is cured it leaves behind silicon nitride, which then acts as the fining agent for the preform. The hope is that through methods such as this one can obtain a still more uniform distribution of holes with even smaller hole sizes.

Another area of research which could be pursued is the development of the use of other gas producing agents. While some of the preforms fabricated in this work did use silicon carbide, this material was not pursued to the point of fabricating useful fiber. It is possible that the development of alternate gas producing agents, might demonstrate significant differences in fiber behavior.

Conclusions Relating to the Properties of Random Hole Optical Fibers

The evidence amassed in the course of this work has shown several trends in the response of RHOF. The properties of the fibers which were observed can be grouped into the following categories:

- Optical Attenuation (Loss)

  There are two trends which are evident in the examination of the optical loss of RHOF. The first is the impact of the purity of the core material. When a core of bulk fused silica was replaced with one fabricated from high purity synthetic silica, the overall loss was

lowered (with the exception of the high loss engendered by the elevated hydroxyl concentration of the synthetic silica.

The second characteristic which has a significantly larger impact on the attenuation of the optical fiber was the geometrical structure of the cladding. As the cladding progresses from a smaller number of larger holes, to a larger number of smaller holes, there is a dramatic reduction in the optical loss (roughly a factor of four greater than that achieved by using a higher purity core).

- Modal Behavior

  As in the case of ordered hole fibers, the RHOF has also demonstrated a significantly reduced number of supported modes for the given core diameter and difference in the average index.

- Pressure and Temperature Sensitivity

  Perhaps the most remarkable property of the RHOF is its response to pressure application. When a compressive force is applied to the fiber (either perpendicular to the axis of propagation, or hydrostatically) a spectrally dependent loss is instilled in the fiber. This has been observed in every RHOF tested. At the same time, one of these fibers was tested for temperature sensitivity, which is commonly associated with pressure sensitivity. The fiber showed no measurable temperature sensitivity over a range of 600 degrees C. The only measurable response to temperature was an abrupt

transition between 200 and 400°C, which is attributed to the burning of the polymeric jacket.

Recommendations for Further Research into the Properties of Random Hole Optical Fibers

There are two areas in which I anticipate potential benefits of further research into the properties of RHOF. The first is in a measurement of the dispersion of the RHOF. The second is in a rigorous analytical analysis of the pressure sensitivity of the RHOF. Given the vast complexity of this structure, such an analysis may have to be done computationally.

Conclusions Relating to Crucible Technique Fibers

From the research conducted into the development of Crucible Technique fibers, one can draw the conclusion that a method has been devised for fabricating optical fibers which were not previously possible. It has been demonstrated that some glasses with vastly differing thermal properties can be successfully integrated into a single fiber. There are some significant limitations to this technique however. These are:

- The crucible technique can only fabricate fibers which have a relatively small final core diameter, in order to prevent the shattering which is a result of residual stress. In the case of the Lead Indium Phosphate cored fibers, this diameter is somewhat less than 8μm.

- The characteristics of the glasses used for the core and cladding still cannot be too dissimilar. For example, the crucible technique does not enable one to produce a fiber with a pure tellurium oxide core in a silica cladding, as the core material boils before the cladding becomes sufficiently soft to be worked.

Recommendations for Future Work on Crucible Technique Fibers

There are two areas in which I anticipate further improvements in the crucible technique of fabricating hybrid fibers. The first is in the development of the suction method of fabricating fibers. This work is already being continued at Virginia Tech, by Nitin Goel. It is possible that with sufficient effort to development, this will become a feasible method for more readily fabricating hybrid preforms.

The second area in which I see the potential for additional research is the impact of depositing a layer of synthetic silica on the interior of the crucible before inserting the core material. It is possible that doing so might yield a fiber with a lower overall loss, by isolating the optical signal from the low purity silica of the crucible itself.

Overall Conclusions Drawn from this Research

In the course of this research it has become evident that there is little, if any merit in the original intent of combining of the these two technologies. While there is no reason to suppose that such a fiber cannot be fabricated it will assuredly not

achieve the goal of acting as a fiber with extreme nonlinear optical efficiency, since the high difference in refractive index between the core and crucible, would preclude the light from ever interacting with the microstructured outer cladding. Despite this it has been amply demonstrated that new varieties of fibers have been successfully produced, and shown to be of high potential value. The characteristics which have been demonstrated by each of the two new varieties of optical fiber are promising and worthy of note. They have the potential to be of great value in the fields of sensing, and active optical components, as well as in producing low cost fibers, with large cores for short transmission distances.